RadioGraphics

Role of MR Imaging of Uterine Leiomyomas before and after Embolization[1]

Sandeep P. Deshmukh, MD • Carin F. Gonsalves, MD • Flavius F. Guglielmo, MD • Donald G. Mitchell, MD

ONLINE-ONLY CME

This journal-based CME activity has been approved for ***AMA PRA Category 1 Credit™****. See www.rsna.org/education/search/RG*

LEARNING OBJECTIVES

After completing this journal-based CME activity, participants will be able to:

- Describe the MR imaging appearances of uterine leiomyoma and its mimics.
- Discuss the role of MR imaging in embolization of uterine leiomyomas.
- List the MR imaging findings that are pertinent to determining the durable success of UFE.

TEACHING POINTS

See last page

Leiomyoma, the most common uterine neoplasm, is composed of smooth muscle with varying amounts of fibrous connective tissue. Most leiomyomas are asymptomatic, but patients may present with abnormal uterine bleeding or bulk-related symptoms. Over the past decade, uterine fibroid embolization (UFE) has been an effective minimally invasive treatment for symptomatic patients. Magnetic resonance (MR) imaging is the most accurate imaging technique for detection and evaluation of leiomyomas and therefore has become the imaging modality of choice before and after UFE. As leiomyomas enlarge, they may outgrow their blood supply, resulting in various forms of degeneration that change their appearance. Leiomyomas are classified as submucosal, intramural, or subserosal. Submucosal and subserosal leiomyomas may be pedunculated, thus simulating other conditions. Understanding the MR imaging appearance of leiomyomas allows differentiation from other entities. The superior tissue contrast of MR imaging allows diagnosis of leiomyomas with a high level of confidence, ultimately leading to a decrease in the number of surgeries performed and thus reducing healthcare expenditures. MR imaging findings that influence the planning of UFE include the location, size, number, and vascular supply of leiomyomas. In addition, MR imaging can be used to assess the success of UFE and evaluate for potential complications.

Abbreviations: GRE = gradient-echo, UFE = uterine fibroid embolization

RadioGraphics 2012; 32:E251–E281 • **Published online** 10.1148/rg.326125517 • **Content Codes:** GU IR MR OB

[1]From the Department of Radiology, Thomas Jefferson University Hospital, 1080A Main Bldg, 132 S 10th St, Philadelphia, PA 19107. Received April 4, 2012; revision requested April 25; final revision received June 1; accepted June 18. For this journal-based CME activity, the author D.G.M. has disclosed financial relationships (see p E279); all other authors, the editor, and reviewers have no relevant relationships to disclose. **Address correspondence to** S.P.D. (e-mail: *Sandeepd1@yahoo.com*).

Introduction

Leiomyomas, also known as fibroids or myomas, are the most common gynecologic neoplasm, occurring in 20%–30% of women of reproductive age. Leiomyomas account for approximately 30% of all hysterectomies performed in the United States; this figure is as high as 50% among black women (1,2). It has been reported that up to 80% of women with leiomyomas are asymptomatic and require no treatment (3). By other accounts, 20%–50% of women with leiomyomas present with symptoms such as menorrhagia, dysmenorrhea, pressure, urinary frequency, pelvic and back pain, dyspareunia, constipation, or obstipation (4).

Hysterectomy and myomectomy are the traditional surgical treatments for symptomatic leiomyomas (5). For well over a decade, uterine fibroid embolization (UFE) has been a popular and effective minimally invasive treatment for symptomatic fibroids. As a percutaneous interventional technique, this procedure may offer the advantages of avoidance of surgical risks, potential preservation of fertility, and shorter hospitalization (6).

Ultrasonography (US) is still the preferred initial diagnostic test for patients with symptomatic leiomyomas. However, magnetic resonance (MR) imaging is the most accurate imaging modality for detection and localization of leiomyomas and their mimics: adenomyosis, solid adnexal masses, focal myometrial contractions, and occasionally uterine leiomyosarcomas. Although more expensive than US, MR imaging may result in lower healthcare costs for women with pelvic pain (7).

Teaching Point

MR imaging can help triage patients to the most appropriate therapy, thereby decreasing the number of unnecessary surgeries (2). This reduction may potentially reduce healthcare expenditures (7). Over time, preprocedure MR imaging is the diagnostic tool of choice for determining patient eligibility for UFE and for assessing potential procedural risk (8,9). Furthermore, MR imaging is also a useful tool for determining treatment outcome and for diagnosing potential complications after UFE.

Teaching Point

In this article, we review use of MR imaging for evaluation of uterine leiomyomas before and after UFE. After some background information on uterine leiomyomas, we describe the MR imaging appearance of leiomyomas, differential diagnosis, and treatment options and discuss the role of MR imaging in UFE.

Background

Prevalence and Incidence

Prospective cohort studies have shown that race, body mass index, and parity are all factors affecting the prevalence and incidence of leiomyomas; however, after adjustment for both body mass index and parity, the factor of race has little effect (10,11). The incidence of leiomyomas increases with age. By age 50 years, the prevalence of leiomyomas is approximately 80% among black women and 70% among white women (10,11). The estimated prevalence of 70%–80% suggests that the vast majority of women will experience uterine leiomyomas during their lifetime.

Histopathologic Features

The cause of uterine leiomyomas is unknown. They are benign neoplasms composed of whorled fascicles of smooth muscle and fibrous connective tissue anchored in the muscular wall of the uterus (12,13). Although there is no true capsule, these tumors are well circumscribed and surrounded by a pseudocapsule (14).

The size of leiomyomas is variable, ranging from microscopic to large tumors that fill the abdomen. Several observations suggest that estrogen and progesterone play an important role in the growth of leiomyomas. Leiomyomas occur in women of reproductive age, often enlarge during pregnancy or during oral contraceptive use, and regress after menopause (5).

As leiomyomas enlarge, they may outgrow their blood supply. The type of degenerative change depends on the degree and rapidity of the onset of vascular insufficiency (14). The result is various types of degeneration: hyaline or myxoid degeneration, calcification, cystic degeneration, red (hemorrhagic) degeneration, or fatty degeneration (15). In most patients, findings of degeneration are rarely related to the clinical symptoms; however, acute degeneration may be associated with pelvic pain or abnormal uterine bleeding.

Classification

Leiomyomas most commonly involve the myometrium of the uterine corpus but may also occur in the cervix (<5% of cases) (16). According to their location, leiomyomas are classified as submucosal, intramural, or subserosal (14). Submucosal leiomyomas are located beneath the mucosal lining and are immediately adjacent to or protrude into the uterine cavity (Fig 1). Intramural leiomyomas are entirely within the wall of the uterus (Fig 2). Subserosal leiomyomas

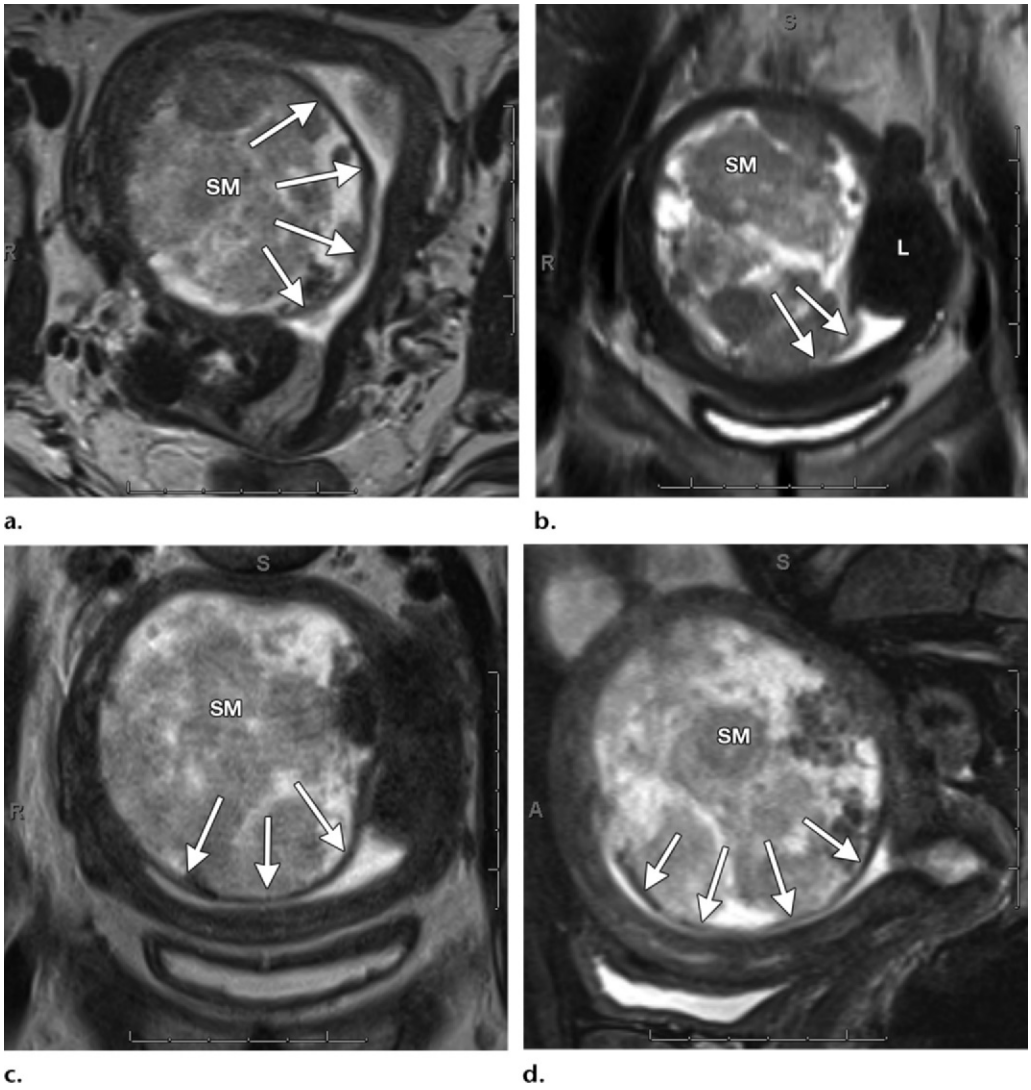

Figure 1. Degenerated submucosal leiomyoma in a 46-year-old woman. Axial **(a)**, coronal **(b)**, oblique coronal **(c)**, and sagittal **(d)** T2-weighted images show a degenerated leiomyoma *(SM)* that is located below the mucosal surface and protrudes into the endometrial cavity (arrows). Also note the nondegenerated submucosal leiomyoma *(L)* in **b**.

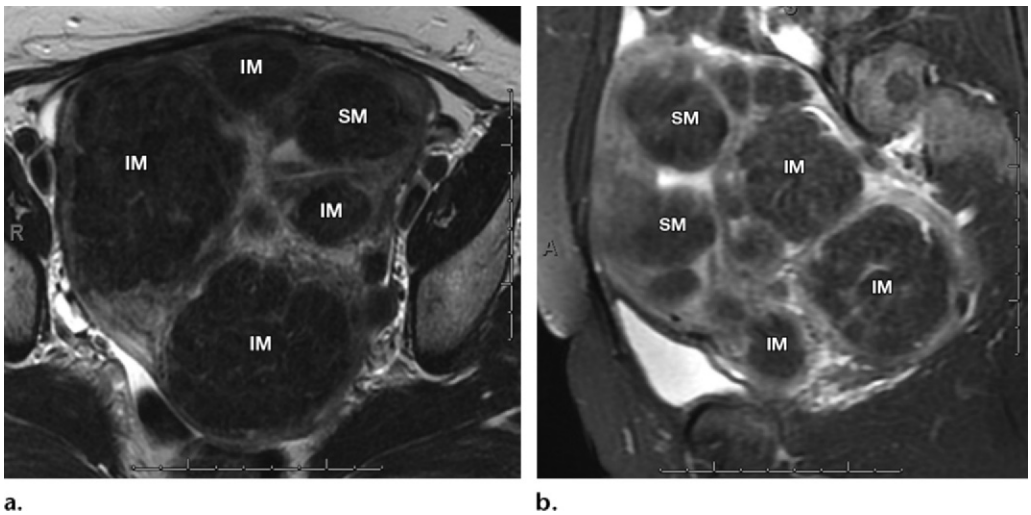

Figure 2. Multiple intramural leiomyomas in a 50-year-old woman. Axial **(a)** and sagittal **(b)** T2-weighted images show multiple intramural *(IM)* and submucosal *(SM)* leiomyomas with decreased signal intensity.

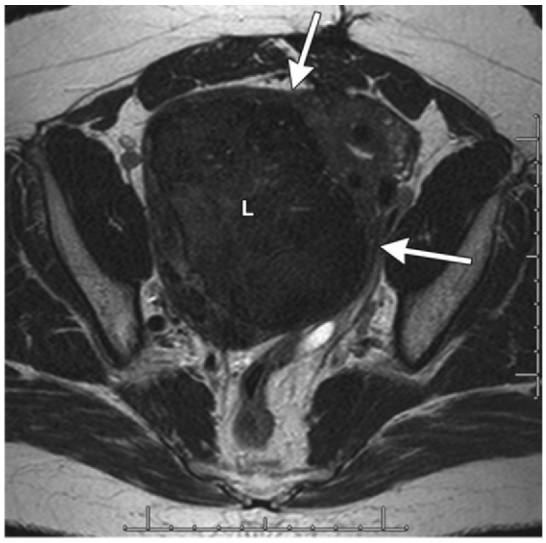

3a.

3b.

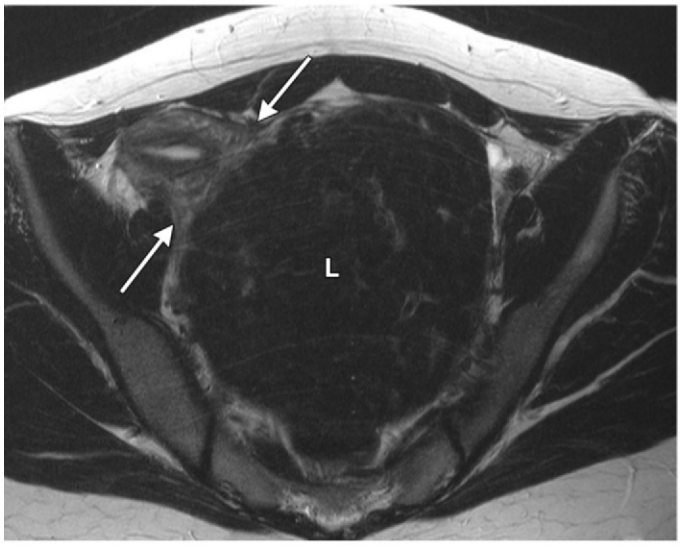

4a.

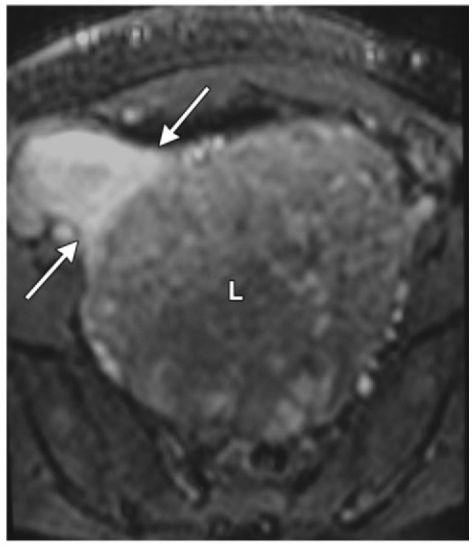

4b.

Figures 3, 4. **(3)** Large broad-based subserosal leiomyoma in a 33-year-old woman. Axial **(a)** and coronal **(b)** T2-weighted images show a large subserosal leiomyoma *(L)* that displaces the uterus and endometrium (*E* in **b**) to the left. Note the myometrial "claws" (arrows) at the base of the leiomyoma. **(4)** Subserosal leiomyoma in another patient. Axial T2-weighted **(a)** and contrast material–enhanced fat-suppressed T1-weighted gradient-echo (GRE) **(b)** images show a broad-based subserosal leiomyoma *(L)*. Myometrial claws (arrows) are noted at the base of the leiomyoma. (Case courtesy of Susan M. Ascher, MD, Georgetown University Hospital, Washington, DC.)

are beneath the uterine serosa and distort the contour of the outer surface of the uterus (Figs 3, 4). Pedunculated leiomyomas are attached to the uterus by a stalk and may be either intracavitary or exophytic (Figs 5, 6).

This classification is of clinical significance because the symptoms and treatment vary among these subtypes of leiomyomas. Although submucosal leiomyomas are the least common, representing only approximately 5% of uterine leiomyomas, they are commonly associated with dysmenorrhea, menorrhagia, or infertility (17,18). Submucosal leiomyomas are clinically described as having the greatest influence on irregular bleeding and infertility because the leio-

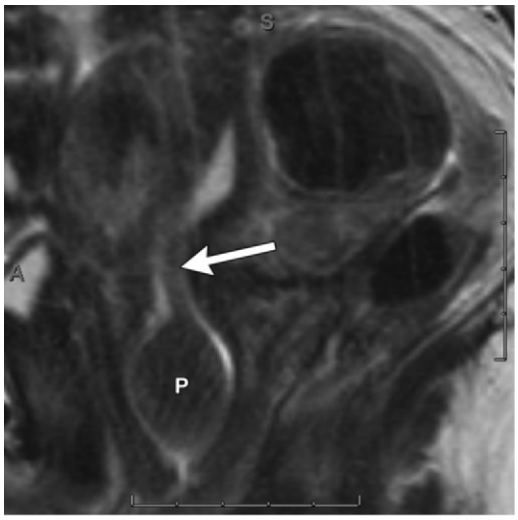

5.

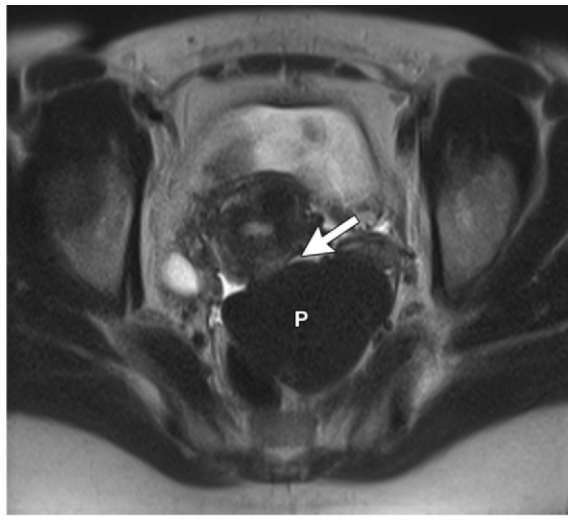

6a.

6b.

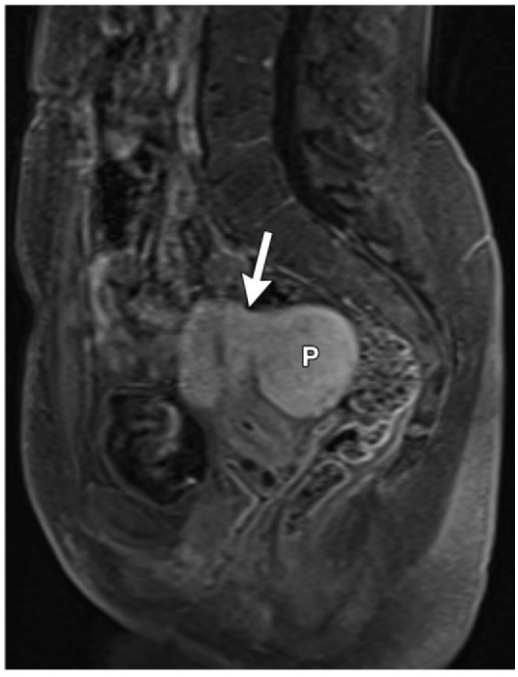

6c.

Figures 5, 6. **(5)** Pedunculated leiomyoma in a 40-year-old woman. Sagittal T2-weighted image shows a pedunculated intracavitary leiomyoma *(P)*, which has prolapsed into the cervix on a long stalk (arrow). **(6)** Pedunculated leiomyoma. Axial **(a)** and sagittal **(b)** T2-weighted and contrast-enhanced fat-suppressed T1-weighted GRE **(c)** images show a pedunculated subserosal leiomyoma *(P)* of the posterior uterine fundus. The leiomyoma is attached by a short stalk (arrow). (Case courtesy of Susan M. Ascher, MD, Georgetown University Hospital, Washington, DC.)

myoma may act as a physical irritant, much like a foreign body in the uterus, interfering with the stability of the endometrium or with successful implantation of the embryo. In rare instances, a submucosal leiomyoma may become pedunculated and protrude into the cervical canal or vaginal canal; the prevalence of such pedunculated submucosal leiomyomas is estimated to be 2.5% (19,20).

Intramural leiomyomas, which are the most common, are usually asymptomatic. However, they can occasionally be associated with menorrhagia and infertility. Infertility can occur secondarily to extrinsic compression of the fallopian tube (21). Menstrual irregularities are hypothesized to be secondary to loss of symmetric uterine contractions (18).

Subserosal leiomyomas are usually asymptomatic; however, pedunculated subserosal leiomyomas may undergo torsion, resulting in infarction accompanied by pain (13). Lateral growth of a subserosal leiomyoma may extend between the folds of the broad ligament (intraligamentous leiomyoma) and simulate an ovarian mass at both clinical and imaging examinations (Fig 7). Rarely, a pedunculated leiomyoma may become attached to an adjacent structure, from which it may derive a new blood supply, and become detached from the uterus (parasitic leiomyoma) (13).

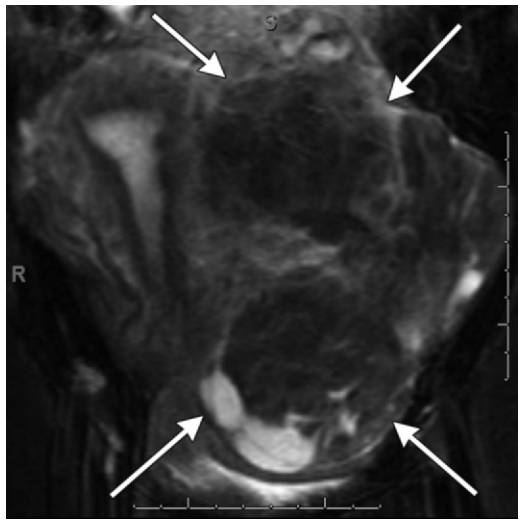

Figure 7. Broad ligament leiomyoma in a 43-year-old woman. Coronal T2-weighted image shows a surgically proved leiomyoma (arrows) of the broad ligament. Although it is difficult to separate the leiomyoma from the uterus, it appears to be centered in the left broad ligament. Differential diagnostic considerations included an exophytic leiomyoma and a broad ligament leiomyoma.

Symptoms

The clinical presentation is variable, depending on the size, location, and number of leiomyomas. Symptoms attributable to leiomyomas can generally be classified into three distinct categories: abnormal uterine bleeding, pelvic pressure and pain, and reproductive dysfunction (22).

Bleeding.—The most frequent symptom of leiomyomas is abnormal uterine bleeding. The bleeding pattern most characteristic of leiomyomas is menorrhagia or menometrorrhagia, excessively heavy or prolonged menstruation. The heavy bleeding can cause medical problems, particularly iron-deficiency anemia. Submucosal leiomyomas are often associated with ulceration of the overlying endometrium and are most likely to cause menorrhagia (22). Bleeding may also be caused by interference of intramural leiomyomas with normal uterine contractility, which presumably plays a role in limiting uterine bleeding during menstruation (18).

Pressure on Adjacent Organs and Pain.—As leiomyomas enlarge, they may produce pressure on surrounding structures. The size of the myomatous uterus is described in menstrual weeks, as is a pregnant uterus. However, unlike the pregnant uterus, the myomatous uterus is irregularly shaped, and specific symptoms can arise from leiomyomas in particular locations. Urinary symptoms can arise from anterior leiomyomas and constipation from those that are posterior. Broad ligament leiomyomas may compress the ureter along the pelvic wall, resulting in hydroureter or hydronephrosis (4).

There is acute pain in the rare cases in which degeneration occurs or there is torsion of a pedunculated leiomyoma. Pain occurs in approximately 30% of women with uterine leiomyomas and is usually the result of acute degeneration (21). Red degeneration, which is most commonly observed during pregnancy, results from hemorrhagic infarction of a leiomyoma. Such degeneration may result in systemic symptoms, such as abdominal pain, low-grade fever, and leukocytosis. Pain may also occur with torsion of pedunculated subserosal leiomyomas or prolapse of pedunculated submucosal leiomyomas.

Reproductive Dysfunction.—Leiomyomas are an infrequent primary cause of infertility. Infertility may be caused by compromise of the patency of the fallopian tube, irritation of the endometrium preventing implantation, or distortion of the endometrial cavity. Tubal obstruction may be caused by intramural leiomyomas located in the cornual regions of the uterus and obstructing the interstitial portions of the tube, or the tube

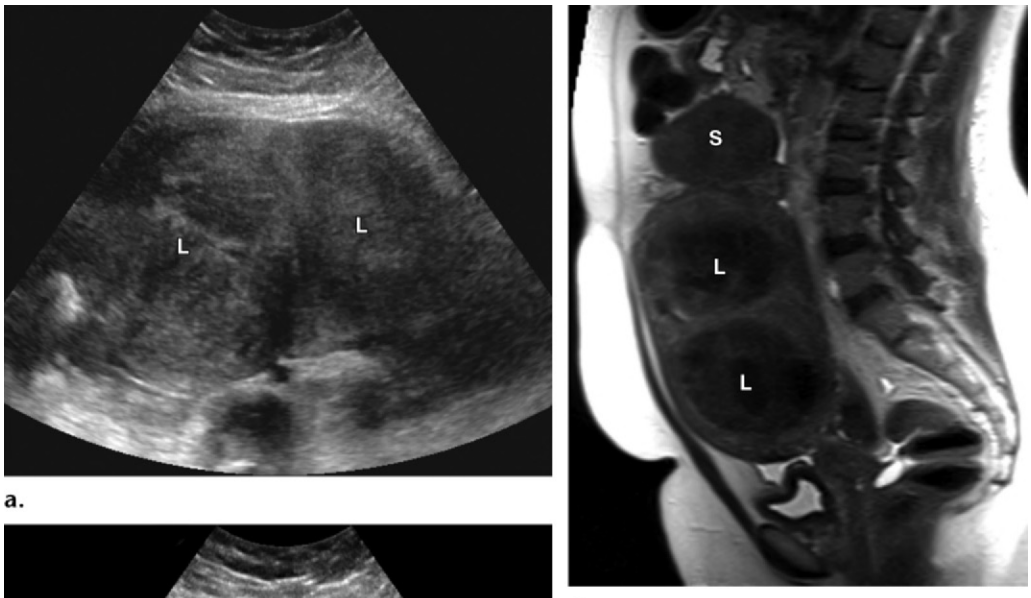

Figure 8. Leiomyomas in a 43-year-old woman being evaluated for UFE. **(a, b)** Transverse **(a)** and sagittal **(b)** transabdominal pelvic US images show a heterogeneously enlarged myomatous uterus. The margins of the leiomyomas *(L)* are not well visualized. **(c, d)** Axial **(c)** and sagittal **(d)** T2-weighted images show multiple intramural leiomyomas *(L)*, as well as an exophytic subserosal leiomyoma (*S* in **d**) arising from the fundus. The subserosal leiomyoma was not identified at US secondary to the limited field of view. The endometrial canal (arrow in **c**) can be seen sandwiched between two of the intramural leiomyomas. (Case courtesy of Susan M. Ascher, MD, Georgetown University Hospital, Washington, DC.)

may be obstructed because of extrinsic compression by leiomyomas located in the broad ligament. Furthermore, patients with submucosal leiomyomas may have an increased prevalence of early abortion resulting from faulty implantation (4). The risk of placental abruption is also substantially increased if the leiomyoma is under the placental site (22).

MR Imaging Appearance of Leiomyomas

MR imaging is considered the most accurate imaging technique for detection and localization of leiomyomas (23). Because of its ability to clearly demonstrate individual tumors, MR imaging is more sensitive than US in detection of leiomyomas (24). The limited field of view of the pelvis during transabdominal and endovaginal US does not consistently allow accurate assessment of the uterus. The excellent soft-tissue contrast of MR imaging provides exquisite detail of uterine zonal anatomy, enabling accurate localization of individual masses as submucosal, intramural, or subserosal (23). MR imaging has been shown to be more accurate than US or hysterosalpingography for determining the presence and location of leiomyomas in infertile women before myomectomy (24) (Fig 8).

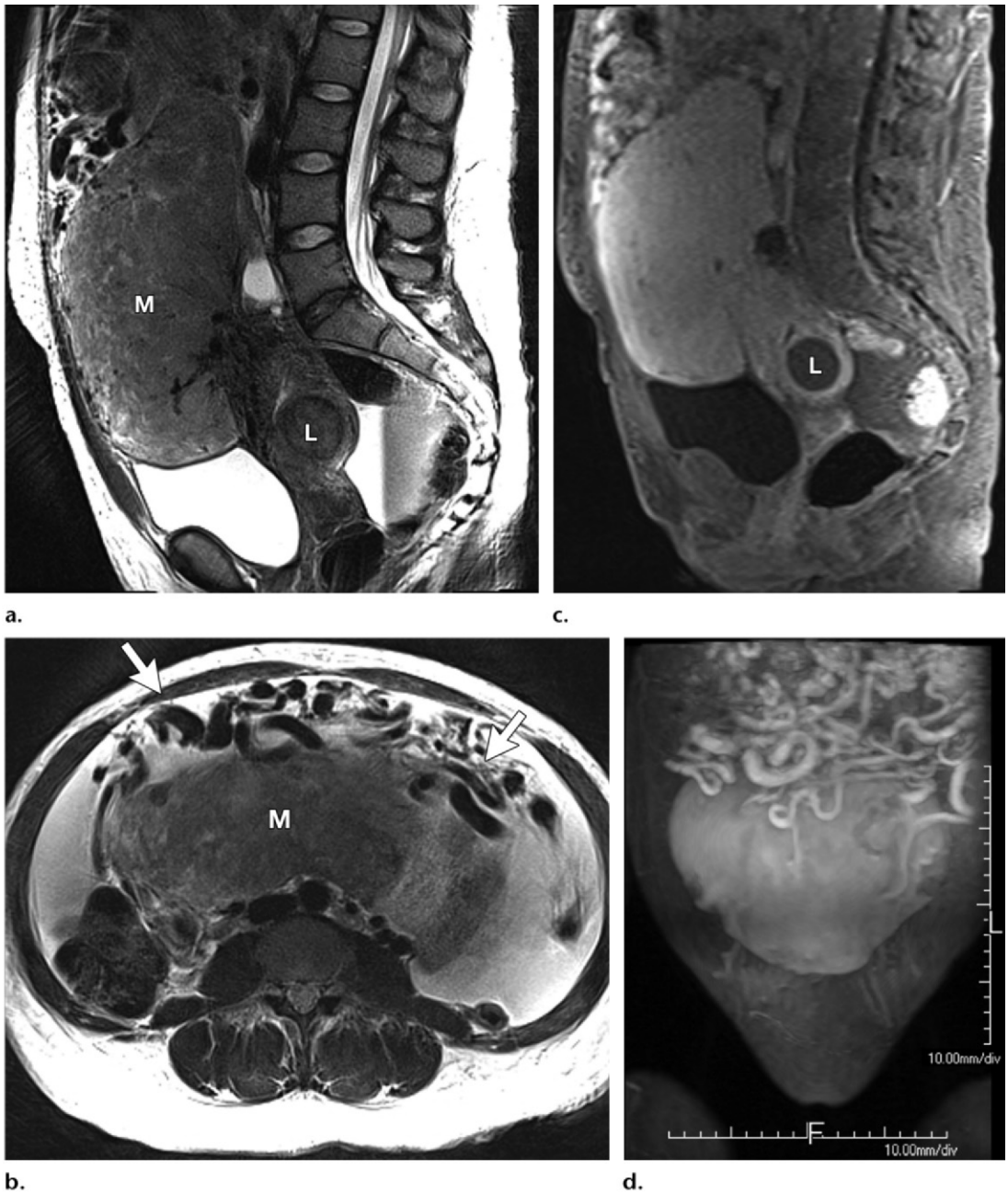

a. c.

b. d.

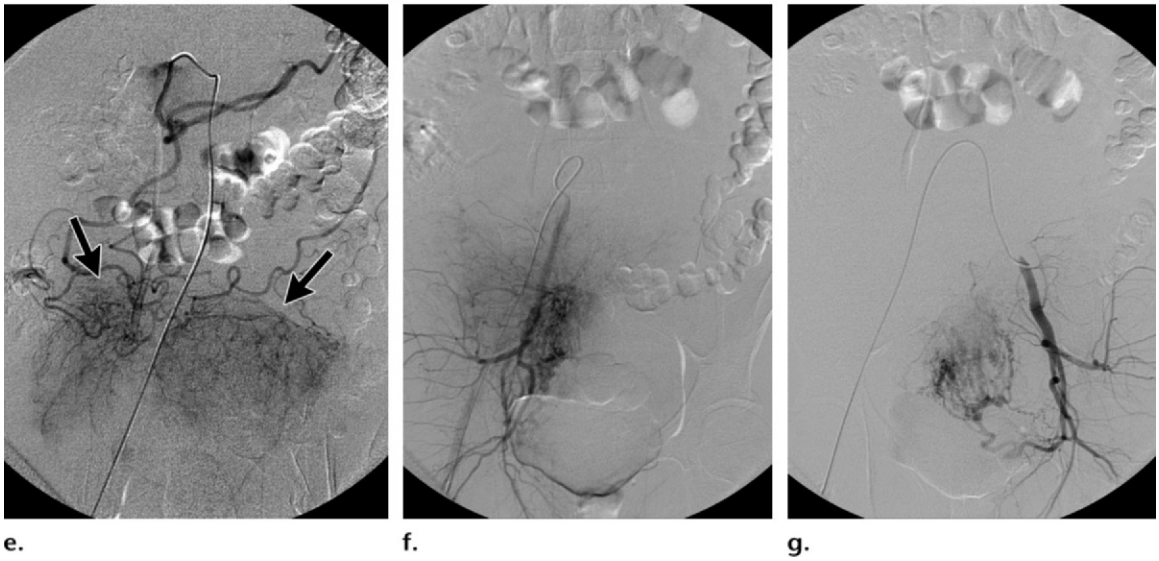

e. f. g.

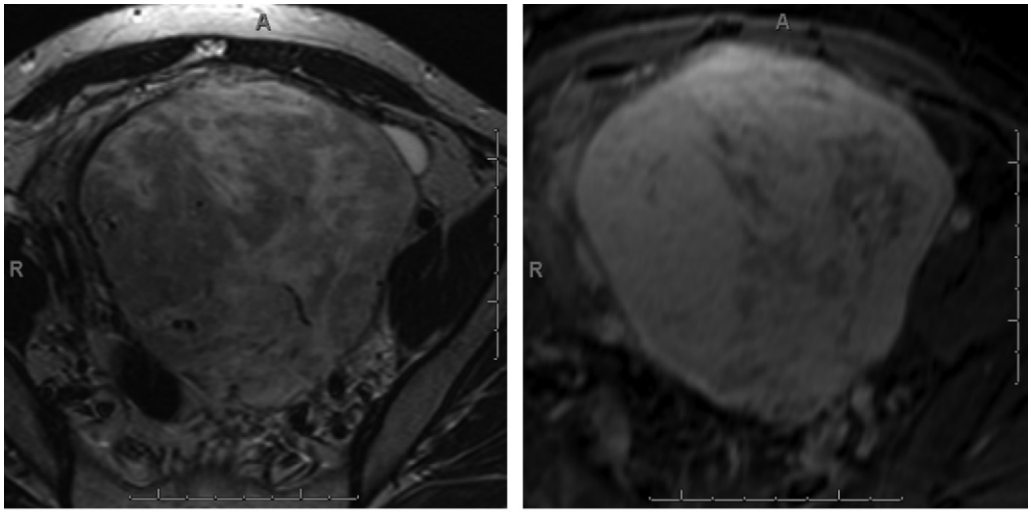

a. b.

Figure 10. Pathologically proved cellular leiomyoma in a 35-year-old woman. **(a)** Axial T2-weighted image shows a large heterogeneous uterine mass with areas of increased signal intensity. **(b)** Axial contrast-enhanced fat-suppressed T1-weighted GRE image shows predominantly homogeneous enhancement of the mass.

Nondegenerated uterine leiomyomas have a typical appearance at MR imaging: well-circumscribed masses with homogeneously decreased T2-weighted signal intensity compared with that of the outer myometrium (23). At histologic examination, nondegenerated leiomyomas are composed of whorls of uniform smooth muscle cells with various amounts of intervening collagen (12). Cellular leiomyomas, which are composed of compact smooth muscles cells with little or no collagen, can have relatively increased T2-weighted signal intensity and demonstrate homogeneous enhancement on contrast-enhanced images (15) (Figs 9, 10).

Degenerated leiomyomas have variable appearances on T1-weighted, T2-weighted, and contrast-enhanced images (15). Low T2-weighted signal intensity is seen in leiomyomas with hyaline or calcific degeneration, an appearance similar to that of standard leiomyomas

◀ **Figure 9.** Cellular leiomyoma in a 42-year-old woman being evaluated for UFE. **(a–c)** Sagittal **(a)** and axial **(b)** T2-weighted and sagittal contrast-enhanced fat-suppressed T1-weighted GRE **(c)** images show a large, enhancing, exophytic uterine mass (*M* in **a** and **b**) with extensive collateral vessels (arrows in **b**). Also note the nonviable uterine leiomyoma (*L* in **a** and **c**). **(d)** Coronal thick-slab maximum intensity projection reformatted image shows extensive collateral vascular supply to the uterine mass. **(e–g)** Celiac axis **(e)**, right internal iliac **(f)**, and left internal iliac **(g)** angiograms show recruited collateral vascular supply (arrows in **e**) to the uterine mass from the gastroduodenal, splenic, and internal iliac arteries. Pathologic analysis demonstrated that the mass was a cellular leiomyoma. (Case courtesy of Susan M. Ascher, MD, Georgetown University Hospital, Washington, DC.)

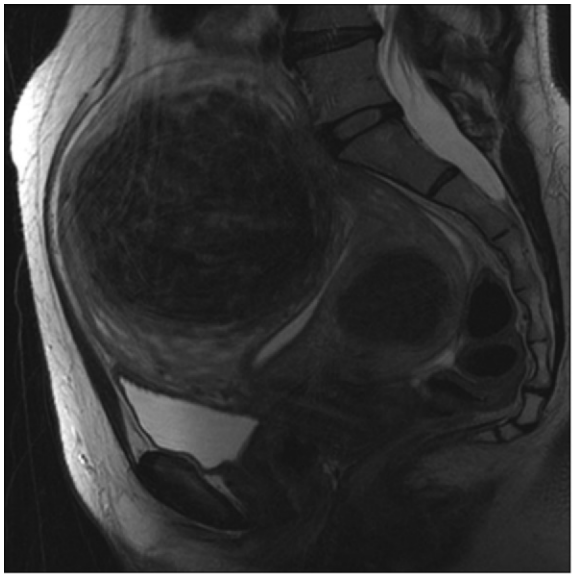

11.

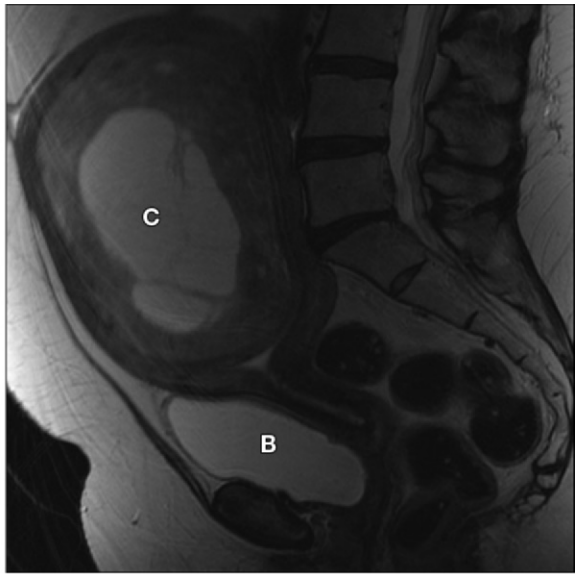

12a.

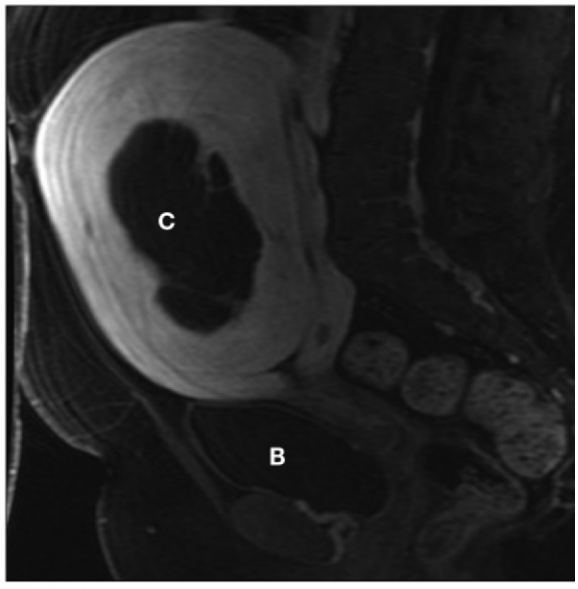

12b.

Figures 11, 12. **(11)** Leiomyomas with hyaline degeneration. Sagittal T2-weighted image shows two intramural leiomyomas with decreased signal intensity, a finding consistent with hyaline degeneration. (Courtesy of Evis Sala, MD, PhD, Memorial Sloan-Kettering Cancer Center, New York, NY.) **(12)** Leiomyoma with cystic degeneration. Sagittal T2-weighted **(a)** and contrast-enhanced fat-suppressed T1-weighted GRE **(b)** images show an intracavitary leiomyoma that has undergone cystic degeneration. Note that the area of cystic degeneration *(C)* does not enhance after intravenous administration of gadolinium contrast material. The enlarged uterus causes mass effect on the urinary bladder *(B)*. (Case courtesy of Evis Sala, MD, PhD, Memorial Sloan-Kettering Cancer Center, New York, NY.)

(Fig 11). Conversely, high T2-weighted signal intensity is seen in leiomyomas with cystic degeneration, and the cystic areas do not enhance (Fig 12). Extremely high T2-weighted signal intensity and minimal contrast enhancement are seen in leiomyomas with myxoid degeneration. Variable T1-weighted signal intensity and low T2-weighted signal intensity are seen in necrotic leiomyomas that have not liquefied (ie, those with hyaline or coagulative necrosis) (15).

Red degeneration (hemorrhagic necrosis) can have an unusual appearance at MR imaging: peripheral or diffuse high signal intensity on T1-weighted images and variable signal in-

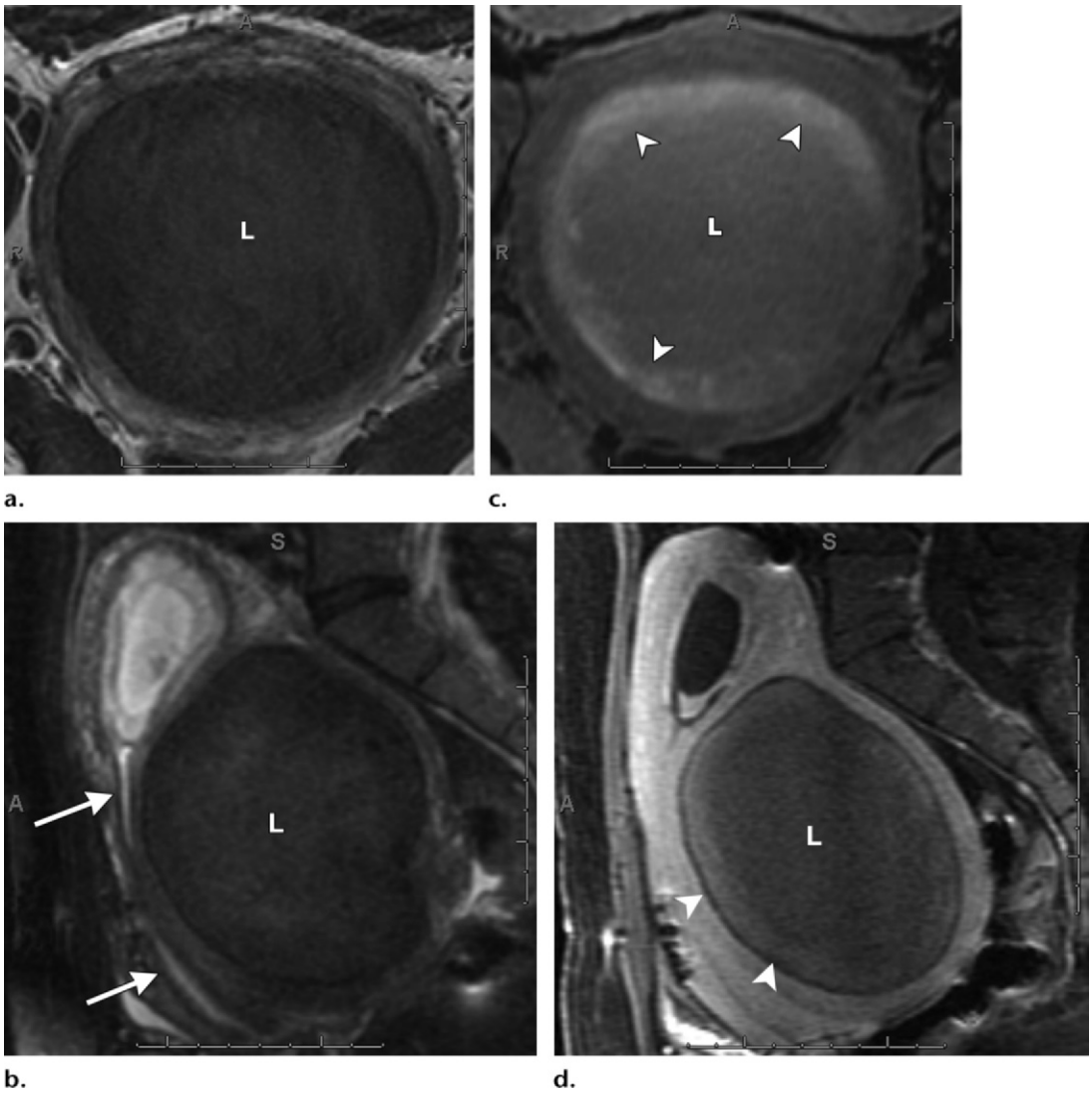

Figure 13. Leiomyoma with red degeneration in a 32-year-old pregnant woman. **(a, b)** Axial **(a)** and sagittal **(b)** T2-weighted images show variable low signal intensity in a large leiomyoma *(L)* of the posterior lower uterine segment. Note the distortion and lengthening of the lower uterine segment and cervix (arrows in **b**) caused by the large leiomyoma. **(c, d)** Axial nonenhanced **(c)** and sagittal contrast-enhanced **(d)** fat-suppressed T1-weighted GRE images of the degenerated leiomyoma *(L)* show peripheral increased signal intensity (arrowheads) and a lack of contrast enhancement.

tensity with or without low signal intensity on T2-weighted images (25) (Fig 13). In red degeneration, methemoglobin or the proteinaceous content of blood results in increased T1-weighted signal intensity (24). When high signal intensity is isolated to the rim of the leiomyoma, it has been hypothesized that the blood products are confined to thrombosed vessels that surround the tumor. Some leiomyomas have a high-signal-intensity rim on T2-weighted images, which

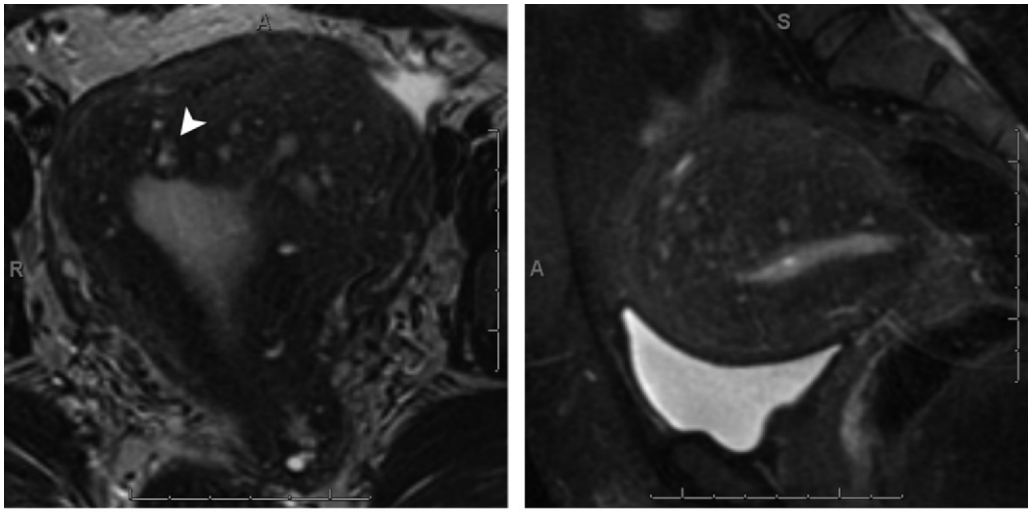

a. b.

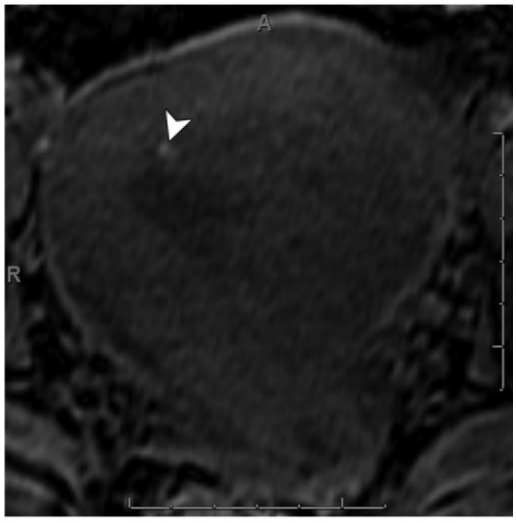

c.

Figure 14. Diffuse adenomyosis in a 39-year-old woman. **(a, b)** Axial **(a)** and sagittal **(b)** T2-weighted images show diffuse thickening of the low-signal-intensity junctional zone with multiple foci of increased signal intensity (arrowhead in **a**), which represent ectopic endometrial glands. **(c)** Axial fat-suppressed T1-weighted GRE image shows high signal intensity in one of the ectopic endometrial glands (arrowhead), a finding consistent with blood products.

represents a pseudocapsule of dilated lymphatic vessels, dilated veins, or edema and corresponds to peritumoral rim enhancement (26,27).

Differential Diagnosis

Other entities can have similar clinical presentations, such as pelvic pain or abnormal uterine bleeding, and therefore need to be distinguished from leiomyomas.

Adenomyosis

Ectopic endometrial glands and stroma within the myometrium with reactive hypertrophy of the surrounding myometrial smooth muscle characterize adenomyosis (28). It is hypothesized that adenomyosis likely results from direct invasion of the basal endometrium into the myometrium, although the cause of such migration is not known. Adenomyosis occurs in focal and diffuse forms, the latter being the more common appearance (28). The clinical manifestations of adenomyosis and leiomyoma are similar in that both may include dysmenorrhea or menorrhagia.

At MR imaging, the diffuse form of adenomyosis appears as a thickened junctional zone (inner myometrium) on T2-weighted images (29). A junctional zone 12 mm thick or thicker is highly predictive of adenomyosis (29). The low signal intensity of adenomyosis on T2-weighted images is due to the reactive, dense smooth muscle hypertrophy that surrounds the imbedded endometrial glands (30). Small foci of high signal intensity on T2-weighted images represent the ectopic endometrial glands. Some of these ectopic

Figure 15. Focal adenomyosis. **(a–c)** Axial **(a)**, oblique axial **(b)**, and sagittal **(c)** T2-weighted images show a focal, ill-defined, poorly marginated area of decreased signal intensity *(A)* in the posterior uterine body. The area of decreased signal intensity is contiguous with the inner myometrium (junctional zone) and contains foci of increased signal intensity (arrowhead in **a** and **b**). **(d)** On an axial fat-suppressed T1-weighted GRE image, one of the foci of increased T2-weighted signal intensity shows corresponding increased T1-weighted signal intensity (arrowhead), a finding consistent with an ectopic endometrial gland containing blood products. Features that favor the diagnosis of focal adenomyosis over that of a leiomyoma include ill-defined margins, foci of high signal intensity, elliptical morphology, and lack of mass effect relative to size.

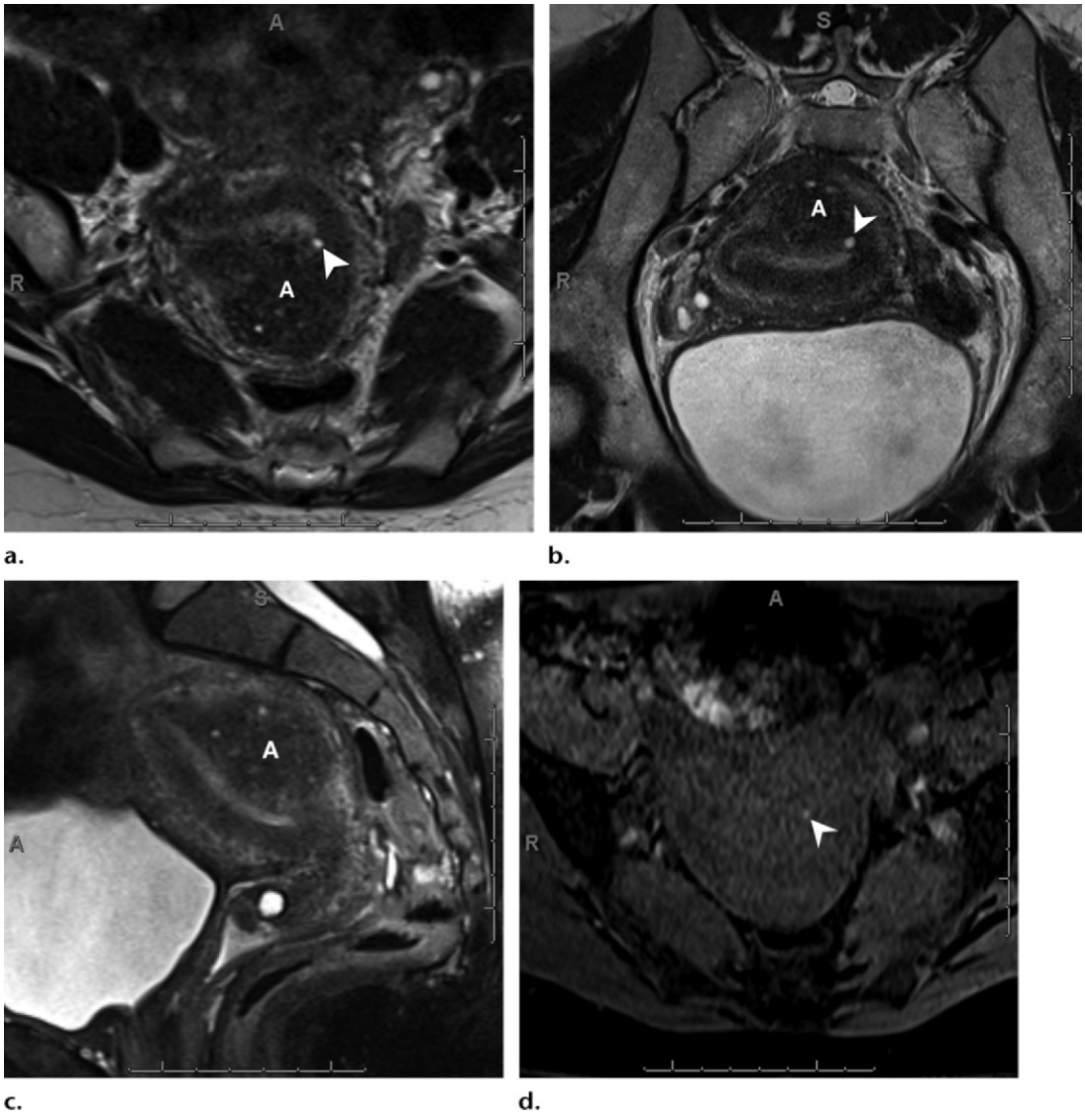

endometrial glands also have corresponding high signal intensity on T1-weighted images, a finding that corresponds to hemorrhage (31,32) (Fig 14).

In its focal form, adenomyosis appears as an ill-defined, poorly marginated area of low signal intensity within the myometrium on T2-weighted images, whereas leiomyomas often appear as well-circumscribed masses (31) (Fig 15). Similar treatment options for adenomyosis and leiomyomas have differing success rates, emphasizing

a. b.

Figure 16. Coexistence of adenomyosis and leiomyomas. Sagittal T2-weighted **(a)** and contrast-enhanced fat-suppressed T1-weighted GRE **(b)** images show a uterus containing adenomyosis (*A* in **a**) and multiple leiomyomas *(L)*. At least one of the leiomyomas is pedunculated *(P)* with a short narrow stalk (arrow in **a**). (Case courtesy of Susan M. Ascher, MD, Georgetown University Hospital, Washington, DC.)

the importance of distinction at preprocedure imaging. MR imaging allows easy differentiation between adenomyosis and leiomyomas. It is important to note that these conditions can coexist (32) (Fig 16).

Solid Adnexal Mass

Adnexal masses and pedunculated leiomyomas can be detected and characterized with MR imaging. If MR imaging can demonstrate continuity of an adnexal mass with the myometrium, even if only by the presence of bridging vessels, then a diagnosis of leiomyoma can be established (33,34) (Fig 17). Owing to the limited field of view in the pelvis at US, depiction of the ovaries can be limited, especially in the case of an enlarged uterus. The ability of MR imaging to demonstrate normal ovaries, even in the presence of an enlarged myomatous uterus, may aid in determining the origin of pelvic masses by allowing exclusion of the diagnosis of an ovarian neoplasm (Fig 18).

Ovarian fibromas and Brenner tumors are benign ovarian neoplasms that have a large fibrous component and can have signal intensity similar to that of a pedunculated leiomyoma (35,36). MR imaging can show fibromas and Brenner tumors surrounded by ovarian stroma and follicles,

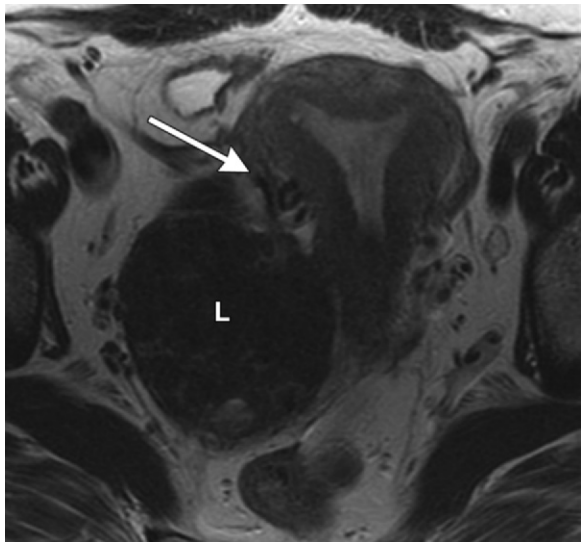

Figure 17. Differentiation of a leiomyoma from an adnexal mass. Axial T2-weighted image shows a broad-based subserosal leiomyoma *(L)* with associated bridging vessels (arrow). The presence of bridging vessels allows the diagnosis of leiomyoma to be made, thereby allowing exclusion of an adnexal mass. (Courtesy of Evis Sala, MD, PhD, Memorial Sloan-Kettering Cancer Center, New York, NY.)

thus establishing the ovarian origin of the mass and allowing exclusion of a diagnosis of leiomyoma (Fig 19). Differentiation between leiomyomas and ovarian adnexal masses is particularly

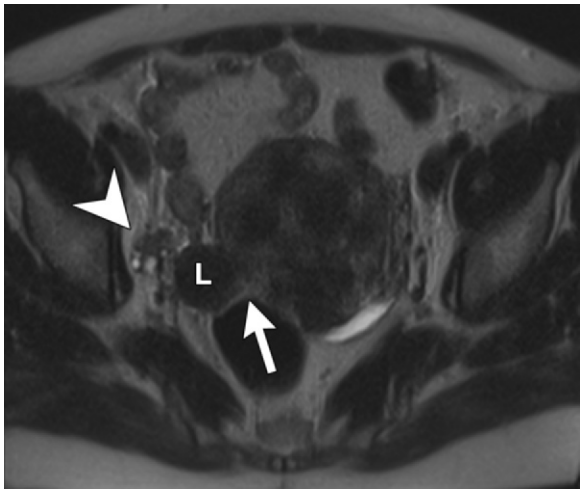

Figure 18. Differentiation of a leiomyoma from an adnexal mass. Axial T2-weighted image shows a broad-based subserosal leiomyoma *(L)* that is contiguous with the uterus (arrow) and separate from the right ovary (arrowhead). These findings allow confirmation of the diagnosis of leiomyoma and not ovarian fibroma. (Courtesy of Susan M. Ascher, MD, Georgetown University Hospital, Washington, DC.)

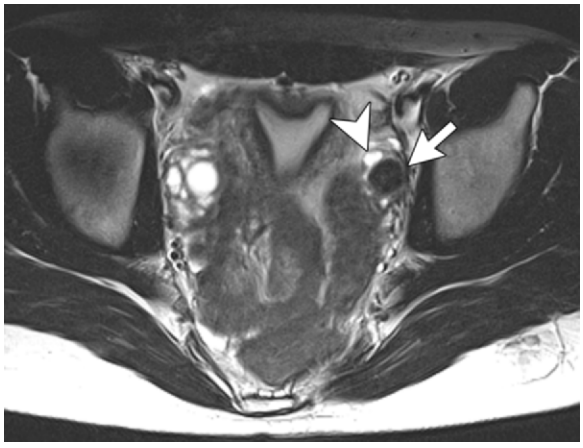

Figure 19. Differentiation of a fibroma from a leiomyoma. Axial T2-weighted image shows a left ovarian fibroma (arrow) surrounded by follicles (arrowhead). The uterus can be identified separately. (Courtesy of Susan M. Ascher, MD, Georgetown University Hospital, Washington, DC.)

important in pregnant patients because confident diagnosis of a leiomyoma may eliminate the need for surgery during pregnancy.

Focal Myometrial Contraction

Uterine contractions can appear as transient hypointense T2-weighted masses and may simulate leiomyomas or focal adenomyosis at MR imaging (Fig 20). Because the contractions are transient, resolution of the mass at subsequent imaging allows the diagnosis to be established (37).

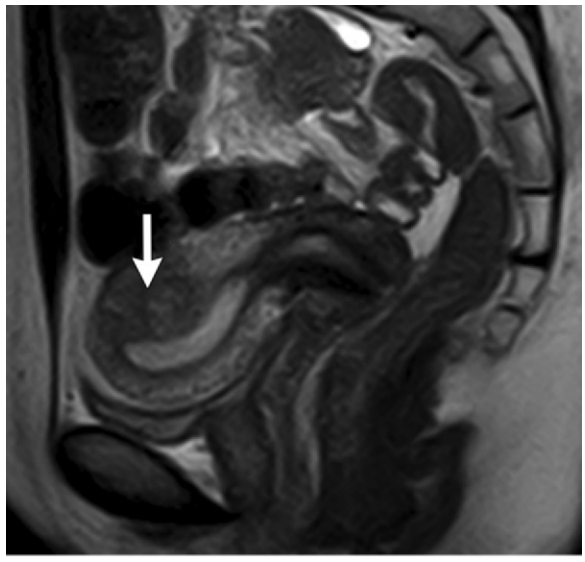

a.

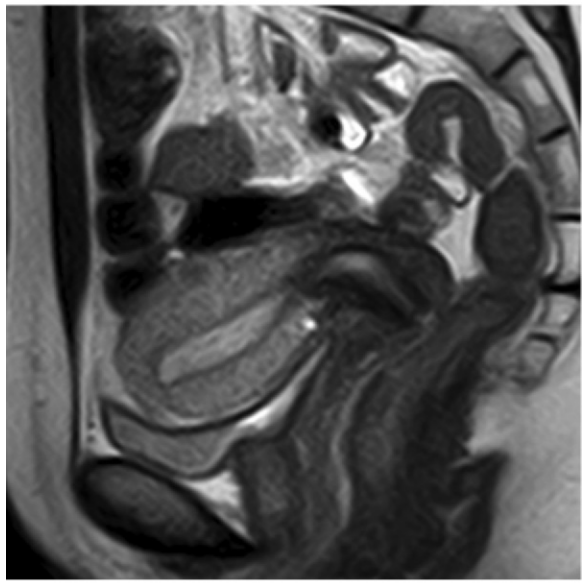

b.

Figure 20. Differentiation of a uterine contraction from a leiomyoma. Sagittal T2-weighted images show a transient uterine contraction (arrow in **a**). (Case courtesy of Kaori Togashi, MD, PhD, Kyoto University, Kyoto, Japan.)

Uterine Leiomyosarcoma

Leiomyosarcomas account for one-third of uterine sarcomas (38). Leiomyosarcomas may arise from the connective tissue of uterine blood vessels, in a preexisting leiomyoma, or de novo from uterine musculature (39). The prevalence of sarcomatous change in benign uterine leiomyomas is reported to be 0.1%–0.8% (40).

Leiomyosarcoma usually manifests as massive uterine enlargement with irregular central zones

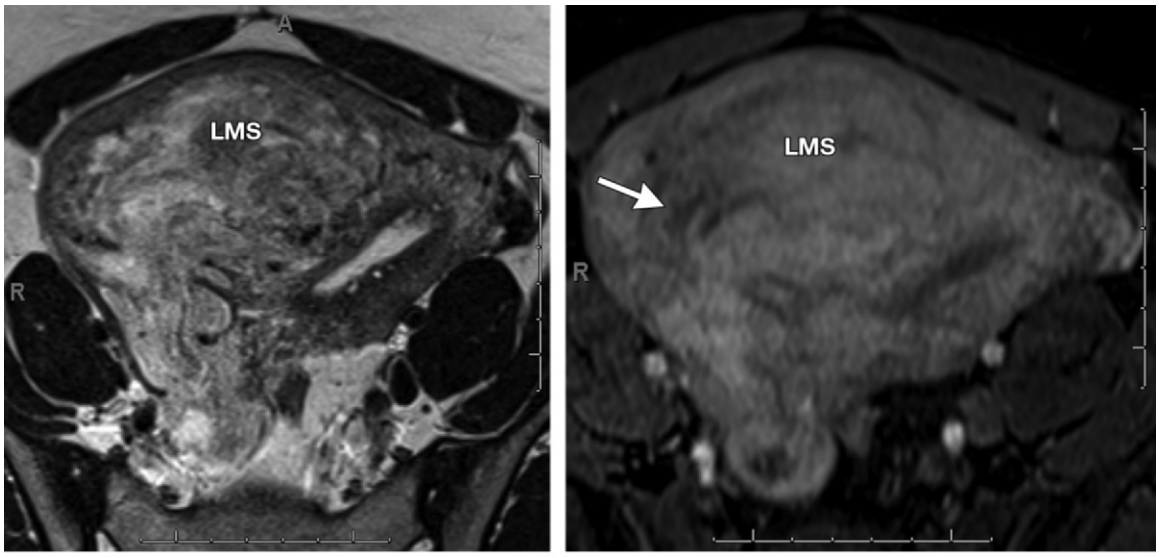

a. b.

Figure 21. Uterine leiomyosarcoma in a 48-year-old woman. Axial T2-weighted **(a)** and contrast-enhanced fat-suppressed T1-weighted GRE **(b)** images show an enlarged uterus containing a heterogeneous mass *(LMS)* with poorly defined margins and internal necrosis (arrow in **b**). Pathologic analysis demonstrated that the mass was a leiomyosarcoma.

of extensive hemorrhage and necrosis (Fig 21). Foci of calcification may be present. It has been suggested that an irregular margin of a uterine leiomyoma at MR imaging is suggestive of sarcomatous transformation, but the specificity of this finding has not been established (39).

Treatment Options for Leiomyomas

Among the women with leiomyomas in the United States, less than one-half will have the diagnosis made by their primary care provider, in part because many women with leiomyomas have no symptoms (41). Once patients become symptomatic, there are multiple therapeutic options available.

Surgical Treatments

Hysterectomy.—Leiomyomas are the leading indication for hysterectomy in the United States (1). The surgery can be performed via the vaginal or abdominal route. In selected cases, the uterus can be removed with a laparoscopic approach.

Myomectomy.—Myomectomy, enucleation of a leiomyoma from the uterine corpus, is indicated in women with a history of second-trimester fetal loss, anemia secondary to hypermenorrhea, or pelvic pain (42). Myomectomy is the second most common surgery performed for leiomyomas in the United States (1). The risk of recurrence after myomectomy has been estimated to be 27% after 10 years (43).

Newer Surgical Techniques.—Developments in surgical endoscopy have, in selected cases, allowed myomectomy to be performed with minimally invasive surgical procedures, including hysteroscopic myomectomy, laparoscopic myomectomy, and laparoscopic myoma coagulation. These procedures offer several advantages, including shorter hospitalization, more rapid recovery, and cost savings per patient in hospital and surgical fees (2).

Nonsurgical Treatments

In the United States, more women receive medical therapy than surgery for relief of symptomatic leiomyomas (44). Pharmaceutical management of symptomatic leiomyomas is most commonly performed as an adjunctive treatment before surgery, since few medications serve as a permanent alternative to surgery.

Gonadotropin-releasing Hormone Analogs.—Gonadotropin-releasing hormone agonists are often used as preoperative adjunctive therapy to surgery. They cause down-regulation of estrogen receptors, which decreases growth of leiomyo-

mas. Therapy with gonadotropin-releasing hormone agonists also helps optimize hematocrit levels, which may have declined secondary to menorrhagia from the leiomyomas. However, after cessation of treatment, there is rapid regrowth of the tumor (45–47).

Uterine Fibroid Embolization.—UFE is a popular and effective method of treating symptomatic leiomyomas. The procedure involves delivery of embolic particles via the uterine arteries to occlude end-arterioles that perfuse the leiomyomas, thus causing necrosis of the leiomyomas. Symptom relief as well as a decrease in the size of the leiomyomas and the uterus overall occur in a majority of patients (48). As a percutaneous interventional technique, this procedure is an option for women who wish to avoid surgery, are poor surgical candidates, or wish to retain their uterus (6).

MR Imaging–guided Focused Ultrasound.—In 2004, the U.S. Food and Drug Administration approved a device that uses MR imaging–guided focused ultrasound to target and destroy leiomyomas. It is intended for premenopausal women who have completed childbearing. Other than medical management, this is the only completely noninvasive treatment option available. The therapy is extremely accurate, as real-time MR imaging is performed during the procedure to map out and confirm that the ultrasound waves are targeting the leiomyoma precisely. Because this is a new technique, long-term outcomes have not been studied (2).

Role of MR Imaging in UFE

Despite its relatively high cost, MR imaging is a noninvasive procedure that allows the diagnosis of leiomyomas to be established with a great degree of confidence and affects patient treatment by reducing the number of unnecessary surgeries (2). This reduction may potentially reduce healthcare expenditures (7). Accurate detection and localization of leiomyomas with MR imaging, as opposed to physical examination and US, can result in planned therapies being changed or obviated (34).

Although US is the initial imaging study in women suspected to have leiomyomas at physical examination, MR imaging is the imaging modality of choice for potential UFE candidates. It allows establishment of patient eligibility for the procedure and exclusion of other causes of abnormal uterine bleeding and pelvic pain. Preprocedure MR imaging has also proved useful in assessing the success of UFE, as well as assessing potential risks for complications (8,9).

Teaching Point

In a study by Spielmann et al (49), results of MR imaging and US in 49 patients before UFE were compared in terms of uterine and leiomyoma size, leiomyoma location, and total number of leiomyomas. The study demonstrated a significant discrepancy in uterine size, leiomyoma location, and number of leiomyomas between the two imaging modalities. In addition, MR imaging results affected clinical management in 11 of 49 patients (22%): Four patients were excluded from UFE, while seven patients underwent UFE after being deemed unsuitable candidates for embolization at initial US evaluation. The authors concluded that MR imaging provides a significant amount of additional information compared with US and affects clinical management in a substantial number of patients, making MR imaging the imaging modality of choice before UFE.

MR Imaging Findings Pertinent to Success of UFE

Pedunculated Leiomyomas.—It is important to diagnose pedunculated submucosal or subserosal leiomyomas with a narrow stalk before UFE. Initially, it was believed that a pedunculated leiomyoma in a subserosal location was a relative contraindication to UFE because of the risk of separation from the uterus. That is, the potential for stalk necrosis and detachment of the leiomyoma could lead to peritonitis, persistent pain, or infection (50). However, it has been shown that for pedunculated subserosal leiomyomas with a stalk diameter of 2 cm or larger, embolization is not associated with an increased frequency of serious complications (9). The stalk diameter should be included in the MR imaging report.

Detachment of pedunculated submucosal leiomyomas into the endometrial cavity may result in transcervical expulsion of necrotic leiomyoma tissue. Furthermore, intracavitary necrotic debris may obstruct the cervix, become infected, and require medical or surgical intervention (50).

Submucosal Leiomyomas.—Occasionally, submucosal leiomyomas can become intracavitary after UFE (Figs 22, 23). Preprocedure MR imaging can help predict which leiomyomas are more likely to become intracavitary after the procedure. Verma et al (51) evaluated the MR

Teaching Point

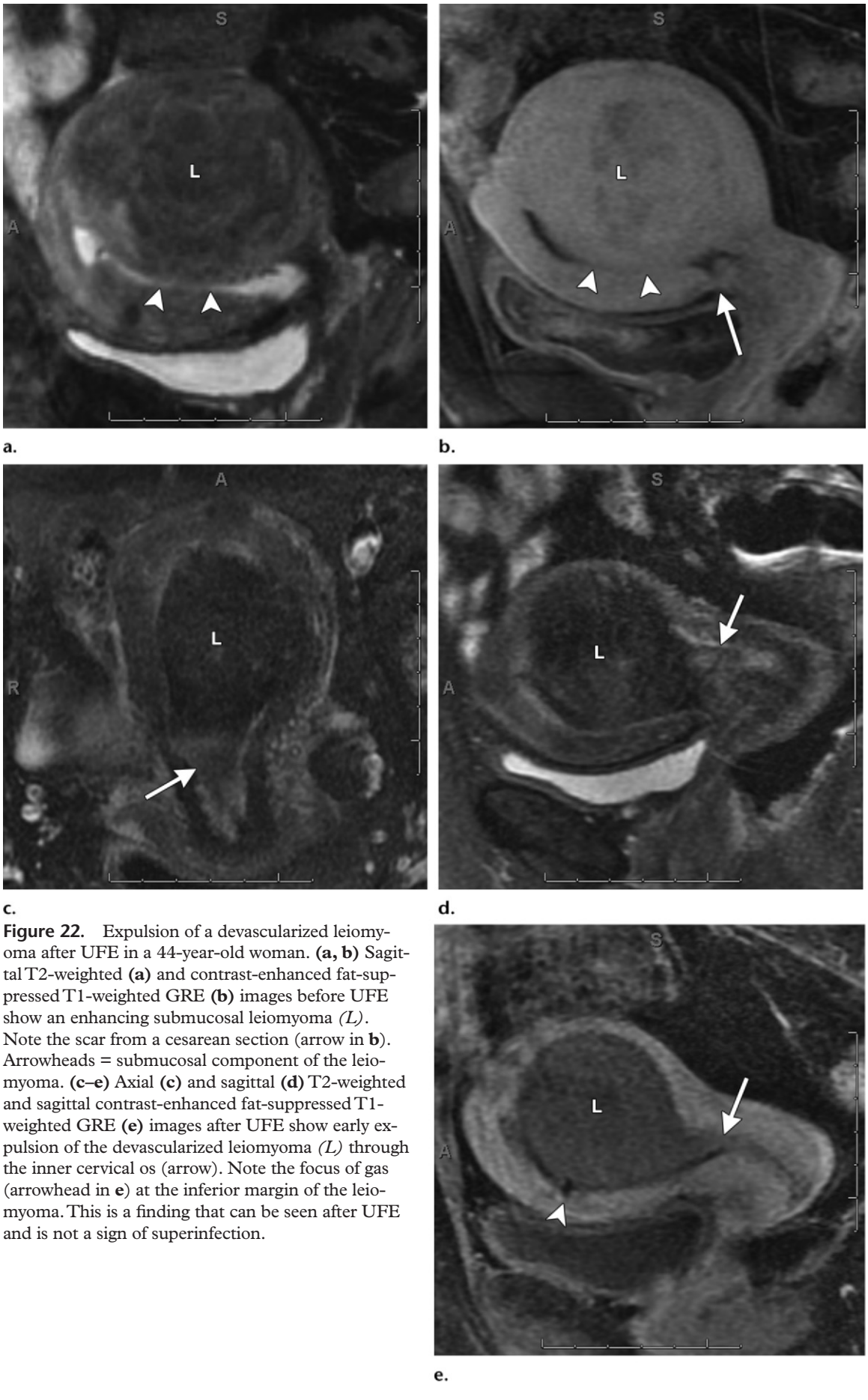

Figure 22. Expulsion of a devascularized leiomyoma after UFE in a 44-year-old woman. **(a, b)** Sagittal T2-weighted **(a)** and contrast-enhanced fat-suppressed T1-weighted GRE **(b)** images before UFE show an enhancing submucosal leiomyoma *(L)*. Note the scar from a cesarean section (arrow in **b**). Arrowheads = submucosal component of the leiomyoma. **(c–e)** Axial **(c)** and sagittal **(d)** T2-weighted and sagittal contrast-enhanced fat-suppressed T1-weighted GRE **(e)** images after UFE show early expulsion of the devascularized leiomyoma *(L)* through the inner cervical os (arrow). Note the focus of gas (arrowhead in **e**) at the inferior margin of the leiomyoma. This is a finding that can be seen after UFE and is not a sign of superinfection.

Figure 23. Submucosal leiomyoma that became intracavitary after UFE in a 40-year-old woman. The leiomyoma subsequently became superinfected and could not be expelled, thus requiring hysterectomy. **(a, b)** Sagittal **(a)** and coronal **(b)** T2-weighted images show a degenerated leiomyoma *(L)* with a large submucosal interface (arrowhead). **(c, d)** Oblique axial **(c)** and sagittal **(d)** T2-weighted images after embolization show that the leiomyoma *(L)* has become intracavitary, with some expulsion of debris (arrowhead) through the cervix. **(e)** Axial T1-weighted image after embolization shows that the intracavitary leiomyoma *(L)* has increased signal intensity, a finding consistent with coagulative necrosis. Note the presence of a broad-based subserosal leiomyoma that has not undergone coagulative necrosis (arrow). **(f)** Sagittal nonenhanced computed tomographic (CT) image shows air (arrowhead) within the superinfected pyomyoma. Note that the bladder *(B)* is difficult to visualize.

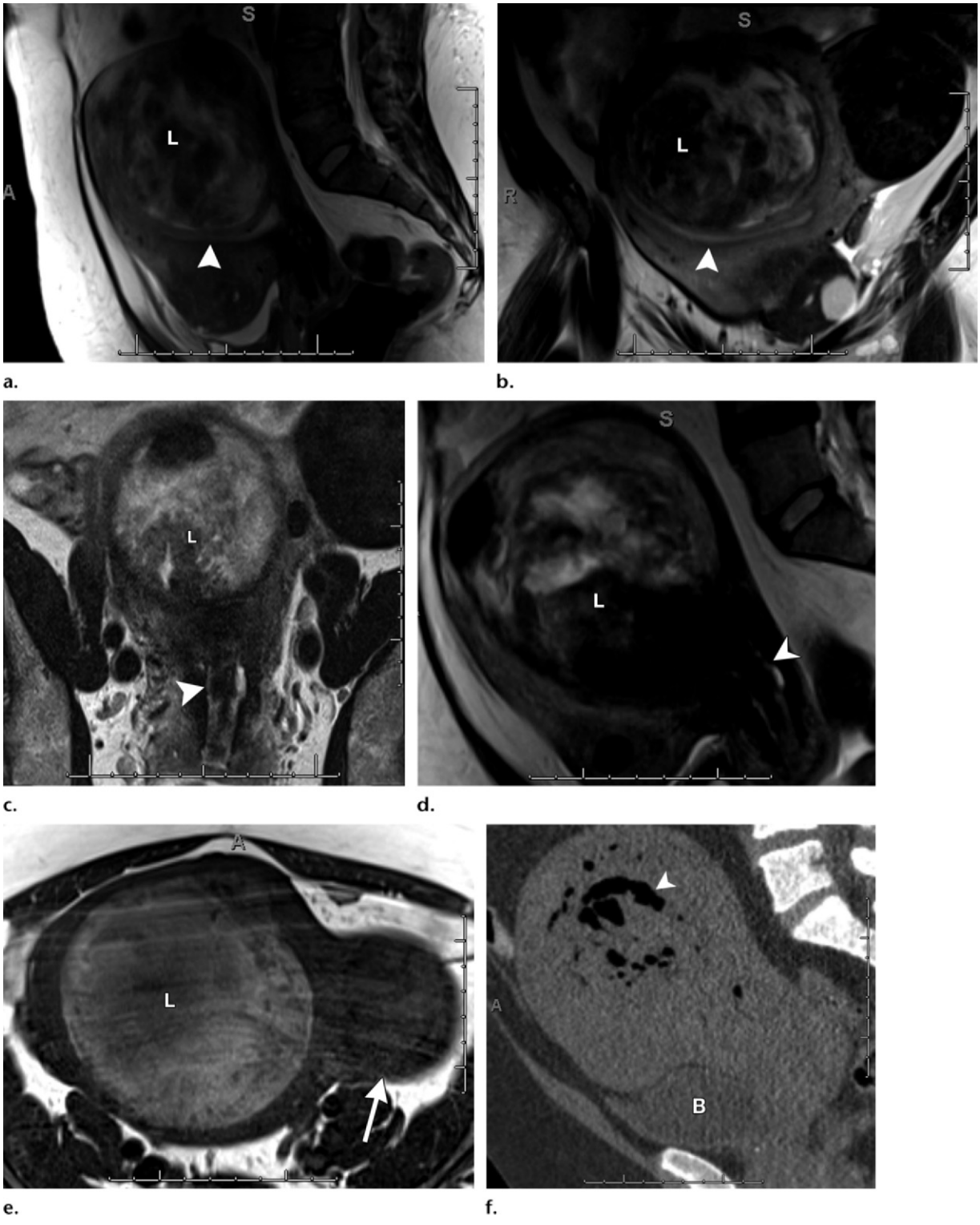

imaging features of 39 submucosal leiomyomas before and after UFE. The ratio of the largest endometrial interface *(I)* to the largest leiomyoma dimension *(D)* was determined with preprocedure MR imaging (Fig 24). Postprocedure MR images were evaluated for a change in the locations of the submucosal leiomyomas.

Thirteen submucosal leiomyomas (33%) became completely or partially intracavitary after embolization. The mean I/D ratio of these leiomyomas was significantly greater than the I/D ratio of leiomyomas that did not become intracavitary after embolization. Furthermore, the mean I/D ratio of the leiomyomas that became completely intracavitary after UFE was higher than the I/D ratio of leiomyomas that became partially intracavitary after UFE. Four of these 13 patients (31%) experienced significant postprocedure symptoms that required further medical or surgical management. The authors concluded that the risk of a submucosal leiomyoma becoming intracavitary after UFE can be determined by assessing the relationship of the size of the leiomyoma relative to its interface with the endometrium by using preprocedure MR imaging.

Expulsion of leiomyomas or fragments of leiomyomas after UFE occurs in up to 10% of cases. Nulliparous women are less likely to pass intracavitary leiomyomas or debris than are multiparous women (52). However, the likelihood of passage of a leiomyoma without the need for further intervention would be relevant information to discuss with a patient before UFE. In another study, Radeleff et al (53) showed that the submucosal leiomyoma expulsion rate is as high as 50% when the volume of the leiomyoma is greater than or equal to 66 mL, which corresponds to a diameter of approximately 5 cm. This information can be used by interventional radiologists to predict which patients may be at risk for potential leiomyoma expulsion or other postprocedure complications.

Nonviable Leiomyomas.—UFE is usually not the best treatment option for patients with symptomatic leiomyomas that do not enhance at preprocedure imaging, since these leiomyomas are already devascularized and therefore less likely to decrease in size after treatment. Thus, these patients' symptoms are less likely to improve after UFE (54).

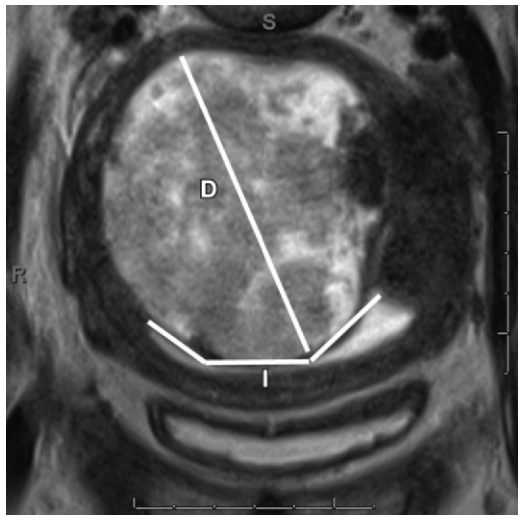

Figure 24. Submucosal leiomyoma in a 46-year-old woman (same patient as in Fig 1). Oblique coronal T2-weighted image shows a submucosal leiomyoma with sample *I* (largest endometrial interface) and *D* (largest leiomyoma dimension) measurements. Note that the endometrial interface distance *(I)* will be calculated by summing the lengths of the line segments.

Cervical Leiomyomas.—Cervical leiomyomas have an alternate blood supply and may not become devascularized after UFE (16) (Figs 25, 26). Research has shown that patients with incomplete infarction of leiomyomas are more likely to have recurrent symptoms related to growth of the uninfarcted tissue (55). Therefore, it is important to determine the presence of cervical leiomyomas at preprocedure MR imaging so that patients can be appropriately counseled about procedural outcomes.

Adenomyosis.—Another advantage of MR imaging is its superiority for diagnosis of adenomyosis and evaluation of the adnexa and endometrium for potential disease, especially when the uterus is enlarged and leiomyomas distort pelvic anatomy. Adenomyosis has been reported in 15%–23% of patients with leiomyomas (56–58). Bazot et al (59) compared MR imaging with transabdominal and endovaginal US for diagnosis of adenomyosis. The sensitivity and specificity of MR imaging and endovaginal US were significantly better than those of transabdominal US for diagnosis of adenomyosis. However, the authors found the accuracy of MR imaging to be superior to that of endovaginal US for identification of adenomyosis in women with concomitant leiomyomas. Identification of adenomyosis before UFE is important because it may affect the clinical success of UFE.

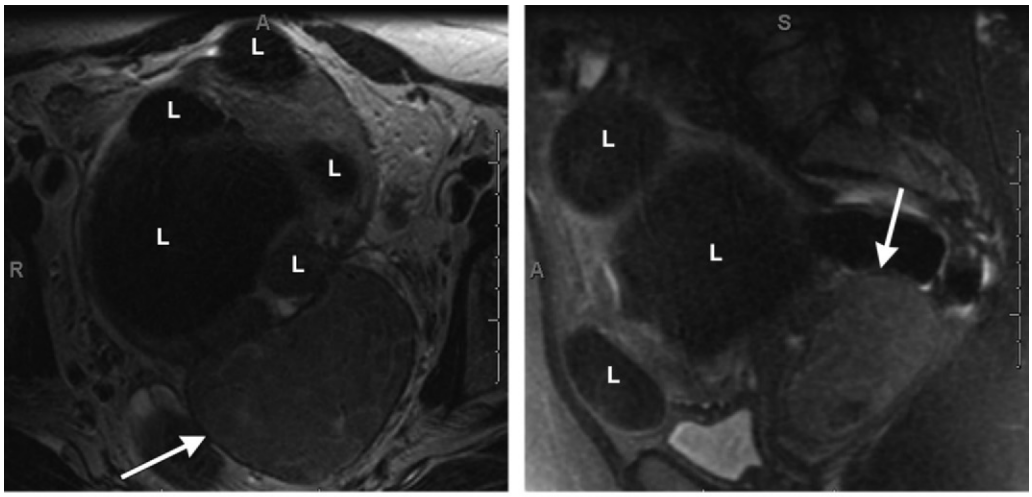

25a.

25b.

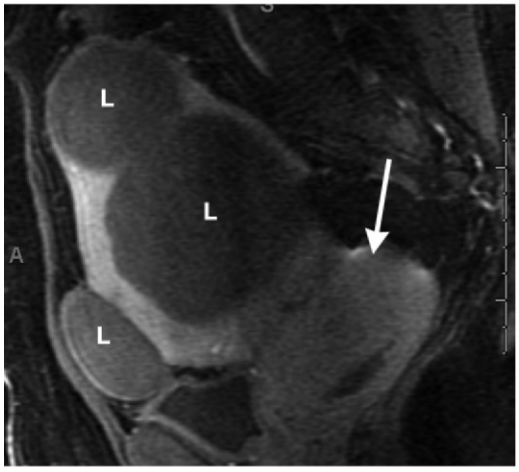

25c.

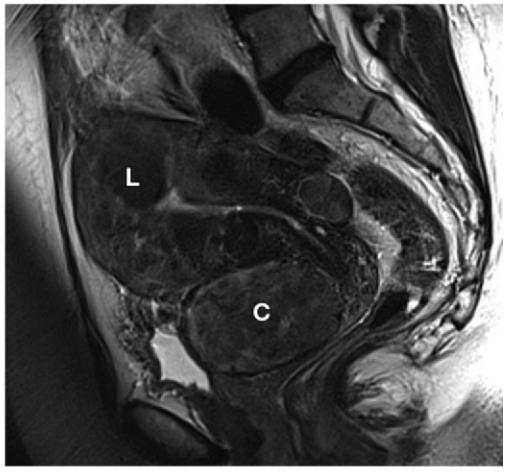

26a.

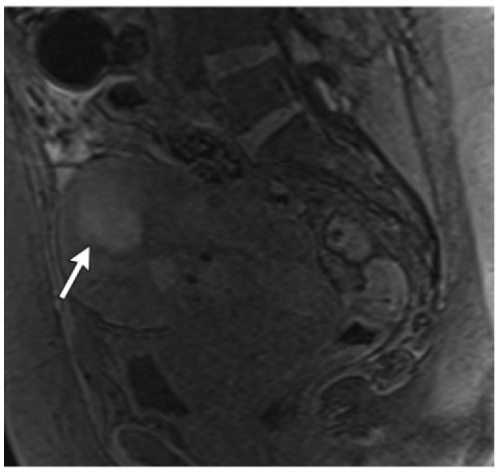

26b.

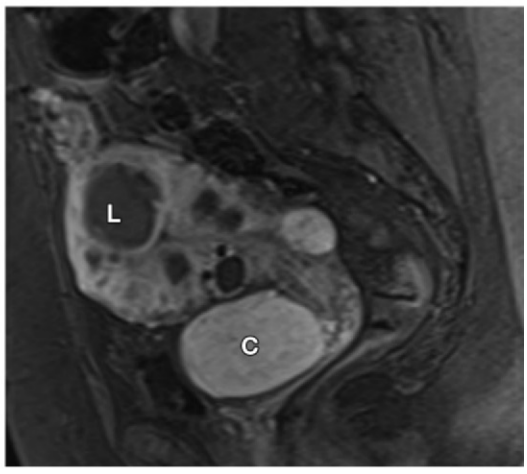

26c.

Figures 25, 26. **(25)** Viable cervical leiomyoma after UFE in a 39-year-old woman. **(a, b)** Axial **(a)** and sagittal **(b)** T2-weighted images show multiple uterine body leiomyomas *(L)* and a cervical leiomyoma (arrow). **(c)** Sagittal contrast-enhanced fat-suppressed T1-weighted GRE image shows lack of enhancement in the devascularized uterine body leiomyomas *(L)* and persistent enhancement in the cervical leiomyoma (arrow) after UFE. **(26)** Viable cervical leiomyoma after UFE. Sagittal T2-weighted **(a)** and nonenhanced **(b)** and contrast-enhanced **(c)** fat-suppressed T1-weighted images show a fundal leiomyoma (*L* in **a** and **c**) that has undergone coagulative necrosis (arrow in **b**) after UFE, with no residual enhancement after intravenous administration of gadolinium contrast material, and a large cervical leiomyoma (*C* in **a** and **c**) that remains viable. (Case courtesy of Susan M. Ascher, MD, Georgetown University Hospital, Washington, DC.)

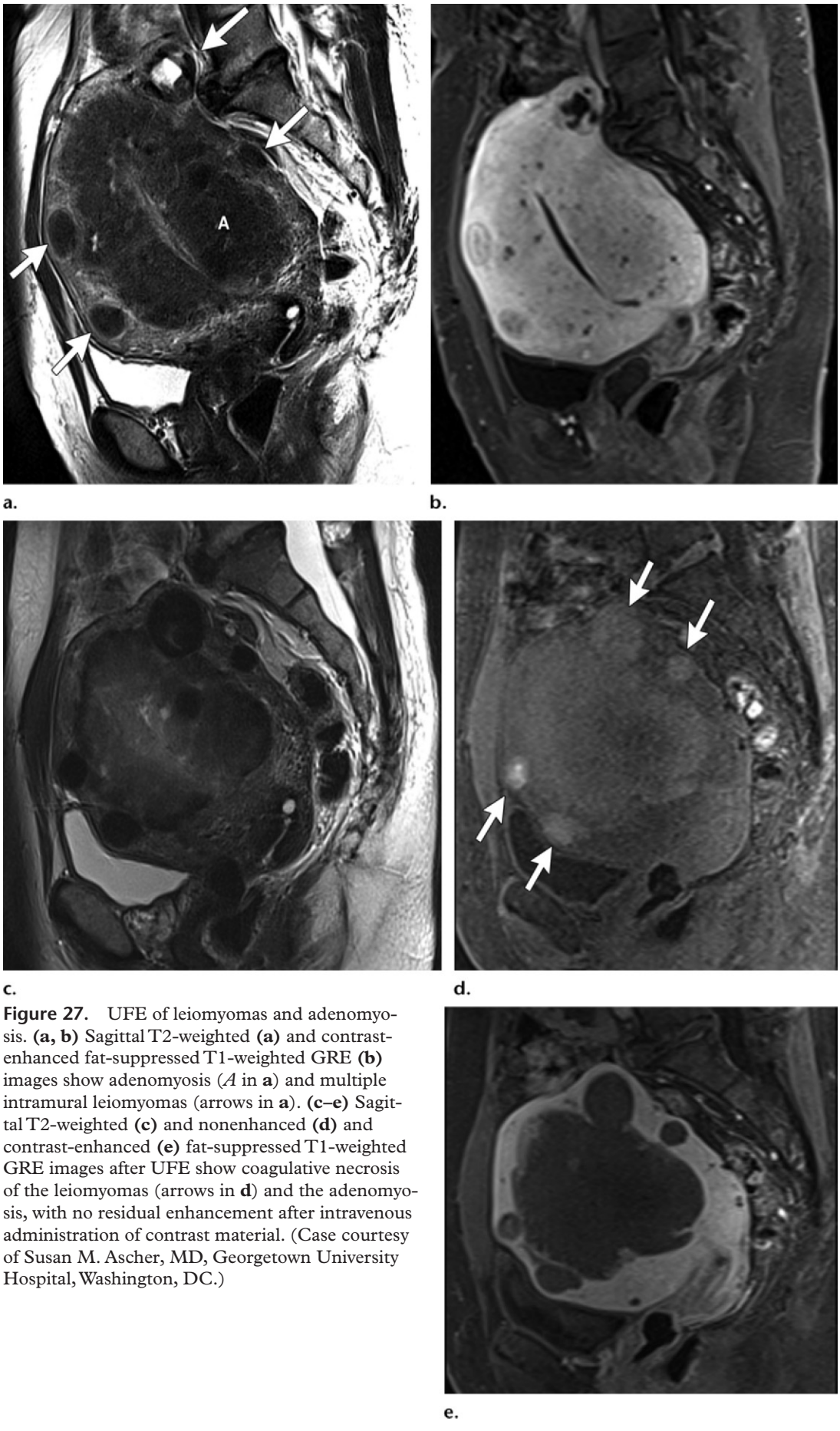

Figure 27. UFE of leiomyomas and adenomyosis. **(a, b)** Sagittal T2-weighted **(a)** and contrast-enhanced fat-suppressed T1-weighted GRE **(b)** images show adenomyosis (*A* in **a**) and multiple intramural leiomyomas (arrows in **a**). **(c–e)** Sagittal T2-weighted **(c)** and nonenhanced **(d)** and contrast-enhanced **(e)** fat-suppressed T1-weighted GRE images after UFE show coagulative necrosis of the leiomyomas (arrows in **d**) and the adenomyosis, with no residual enhancement after intravenous administration of contrast material. (Case courtesy of Susan M. Ascher, MD, Georgetown University Hospital, Washington, DC.)

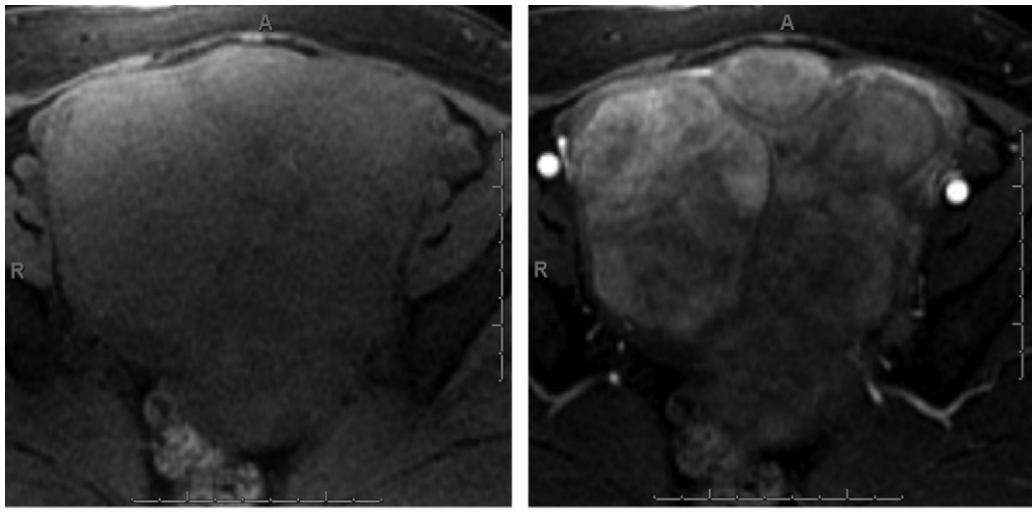

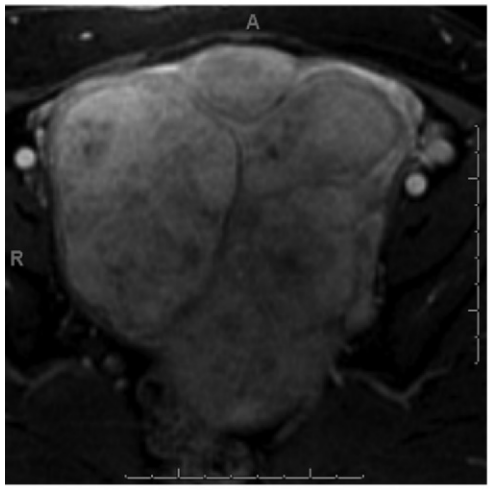

Figure 28. Use of dynamic MR imaging to demonstrate extent of leiomyoma enhancement in a 50-year-old woman. Nonenhanced axial dynamic three-dimensional fat-suppressed T1-weighted image **(a)** and corresponding images from earlier **(b)** and later **(c)** contrast-enhanced phases show dynamic enhancement of multiple leiomyomas.

In a study by Pelage et al (56), 18 women with menorrhagia due to adenomyosis were treated with UFE. Six months after UFE, 94% of the women reported improvement in their menorrhagia; however, 2 years later, 44% of the patients had recurrent symptoms that required additional treatment or hysterectomy. Therefore, it is important to inform patients of the presence of adenomyosis before UFE because adenomyosis may be a potential reason for UFE failure. Although embolization is considered a less optimal treatment for adenomyosis than for leiomyomas, it has been shown that most patients with adenomyosis have symptom relief after UFE, although the rate is not as high as in those with symptoms related to leiomyomas (60,61) (Fig 27).

Pre-UFE MR Imaging Protocol

By using a standard phased-array surface coil, imaging of the pelvis with suspended respiration can be completed in approximately 20 minutes. All protocols should include T2-weighted images in at least two orthogonal planes (generally axial and sagittal) to identify the uterine axis and localize leiomyomas and other uterine disease. Imaging in a third orthogonal plane can be performed to clarify and confirm the findings from imaging in the other two planes. In one of these planes, the T2-weighted images can be obtained with a single-shot technique to conserve time. Axial T1-weighted images, opposed-phase GRE or fast spin-echo, should be obtained to identify the relationship of the leiomyoma to the uterus and adnexa. In addition, these T1-weighted images allow characterization of blood and fat to facilitate diagnosis of concurrent uterine and adnexal disease.

Dynamic three-dimensional nonenhanced and contrast-enhanced fat-suppressed GRE images should be obtained to determine the extent of leiomyoma enhancement and define periuterine vessels (54). This dynamic sequence can be modified to serve as MR angiography, often in the sagittal plane to facilitate identification of parasitized ovarian vessels; however, this can also be performed in the axial plane with similar delineation, although the origin of these vessels may not be included in the imaged volume (Fig 28). In recent years, diffusion-weighted imaging has become more robust for problem solving in the abdomen and pelvis. Diffusion-weighted imaging can also be included to further enhance characterization of leiomyomas and differentiation from other entities (62).

Features That Should Be Reported in Cases of Uterine Leiomyoma

Feature	Description
Size of uterus	Maximal dimensions including the cervix
Number of leiomyomas	Rough estimate of the number of leiomyomas
Location of each leiomyoma	Intracavitary, submucosal, intramural, subserosal, or exophytic
Size of leiomyomas	Maximal dimensions of the three largest index lesions
Size of stalk if pedunculated	Size of the base of the stalk
Extent of interface if submucosal	Size of the submucosal interface
Enhancement characteristics	Percentage of the leiomyoma that enhances
Presence of adenomyosis	Thickness of the inner myometrium and presence of ectopic endometrial glands
Presence of ovarian vessel parasitization, adnexal masses, or endometrial abnormalities	...

Image Interpretation

Teaching Point

The location, size, and enhancement of leiomyomas provide significant prognostic information about the potential success of UFE (54). Therefore, the location, size, size of the stalk (if pedunculated), and enhancement characteristics of leiomyomas should be analyzed and reported (9) (Table). In addition, if there is significant parasitization of ovarian vasculature, consideration may be given to embolizing the ovarian vasculature at the time of UFE, or perhaps at a later date if there is not significant symptom relief after UFE (63) (Fig 29).

If the leiomyomas are already autoinfarcted at preprocedure imaging, the patient is unlikely to benefit from UFE, since the leiomyomas are less likely to decrease in size after the procedure (54). Therefore, hysterectomy or myomectomy may be better options if the patient's symptoms are likely due to bulk effect.

Although the diagnosis of leiomyosarcoma is made on a histologic basis, factors such as irregular shape, ill-defined margins, and internal necrosis can be clues to the presence of a uterine sarcoma. Therefore, these imaging appearances should prompt consideration of surgical management, biopsy before embolization, or short-interval follow-up imaging; continued growth after embolization is an important additional sign of possible malignancy (64).

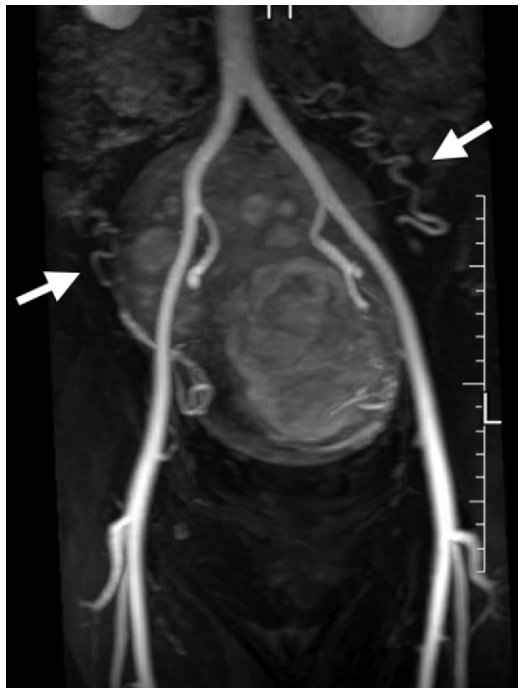

Figure 29. Parasitization of ovarian vasculature. Arterial phase maximum intensity projection MR angiogram before UFE shows bilateral ovarian arterial collateral vessels (arrows). (Courtesy of Susan M. Ascher, MD, Georgetown University Hospital, Washington, DC.)

Comorbid or Alternative Conditions

Nonviability of leiomyomas before UFE decreases the likelihood of benefit for the reasons outlined earlier (54). In addition, comorbid conditions that may preclude UFE include uterine or leiomyoma size (>20 cm), pedunculated leiomyomas with stalks less than 2 cm in diameter, large intracavitary or submucosal leiomyomas, and presence of endometrial or adnexal neoplasms (54).

Outcomes of UFE

Serial follow-up data demonstrate that greater than 70% of patients have symptom relief 5 years after UFE (65). Most of these patients have a decrease in leiomyoma volume; however, the most convincing finding after UFE is coagulative necrosis (ie, hemorrhagic infarction) (8). Trials comparing UFE and surgery demonstrated faster recovery after UFE and good long-term

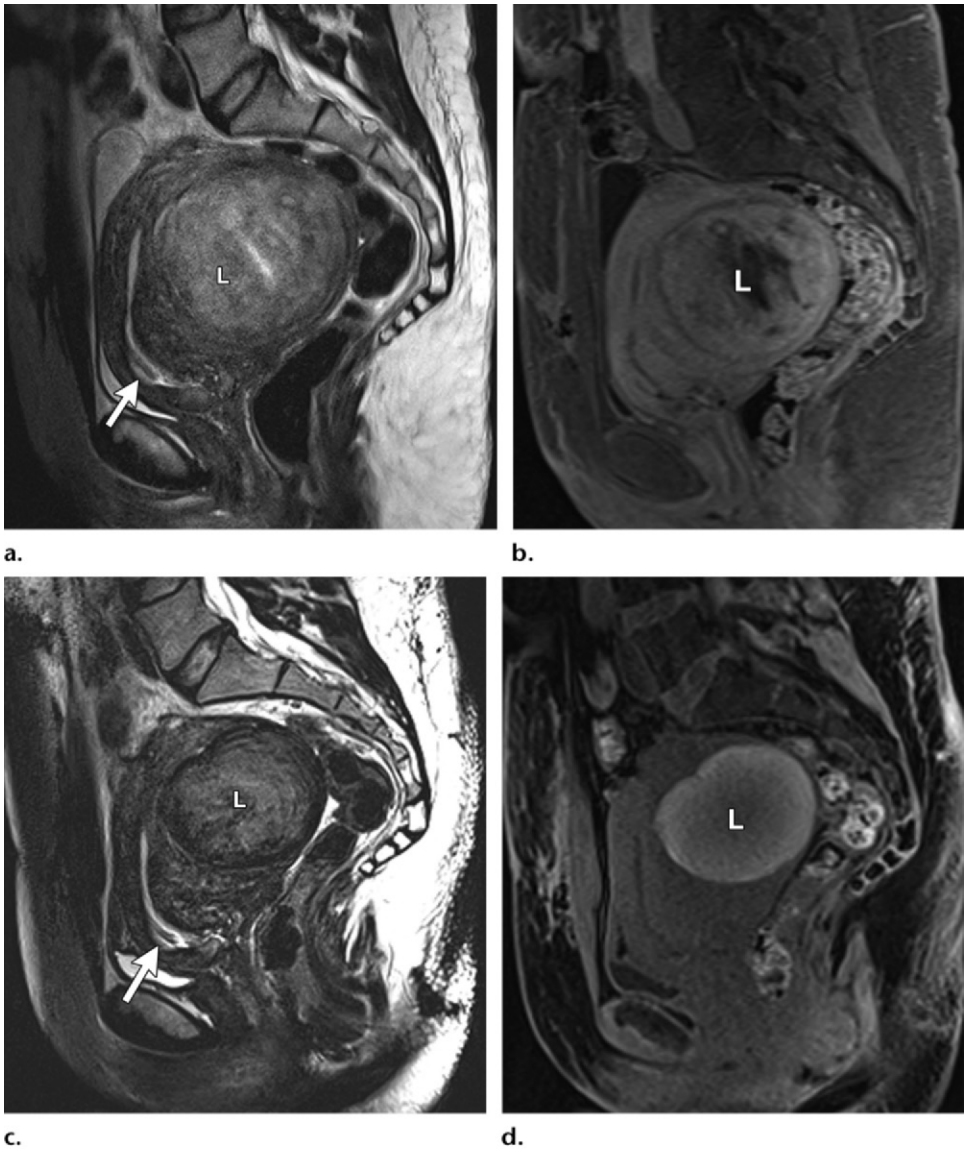

Figure 30. Complete coagulative necrosis. **(a, b)** Sagittal T2-weighted **(a)** and contrast-enhanced fat-suppressed T1-weighted GRE **(b)** images before UFE show a viable intramural leiomyoma *(L)* in the posterior fundus. **(c–e)** Sagittal T2-weighted **(c)** and nonenhanced **(d)** and contrast-enhanced **(e)** fat-suppressed T1-weighted GRE images after UFE show complete coagulative necrosis of the leiomyoma *(L)* without residual viable tissue. Also note the small incidental lower uterine segment polyp protruding into the endocervical canal (arrow in **a** and **c**). (Case courtesy of Susan M. Ascher, MD, Georgetown University Hospital, Washington, DC.)

outcomes, thus establishing UFE as a well-established alternative to hysterectomy about which patients should be informed (66–68).

Post-UFE MR Imaging Surveillance

In patients who become asymptomatic, further imaging may not be necessary. However, MR imaging can be used to reassess for residual enhancement of leiomyomas in patients with continued symptoms, who possibly require reembolization or therapy for a parasitized vessel (commonly the ovarian artery) (7). In addition, patients can be evaluated for passage of leiomyomas (64).

Routine follow-up MR imaging will ideally show complete infarction of uterine leiomyomas, which is demonstrated on MR images as lack of enhancement after contrast material administration (Figs 22, 30). This is sometimes associated with T1-shortening effects of methemoglobin and variable signal intensity on T2-weighted images, depending on the age of hemorrhage within the leiomyoma, a condition known as hemorrhagic

infarction (69) (Figs 23c–23e, 30). Occasionally, a small amount of gas may be identified within a leiomyoma after embolization; this does not equate with a pyomyoma (Fig 22e).

Images should be interpreted in conjunction with the clinical symptoms. With increasing time between UFE and MR imaging, there is progressive liquefaction of leiomyomas with increased signal intensity on T2-weighted images. Leiomyoma calcification typically occurs at least 6 months after UFE and will be seen as low signal intensity on T1- and T2-weighted images along with blooming on GRE images (69).

The goal of UFE is 100% infarction of uterine leiomyomas to achieve optimal and extended improvement in preprocedure symptoms. Residual viable leiomyoma tissue may result in failure of UFE due to regrowth of uterine leiomyomas (55,67) (Fig 31).

Post-UFE Complications

Although rare, complications after UFE have been reported. MR imaging may aid in diagnosis or exclusion of several postprocedure complications. Minor complications include hematoma, transient pain or postembolization syndrome, and delivery of a leiomyoma (64). A hematoma after UFE is rare and manifests similarly to hematomas after other interventional procedures that require arterial puncture.

Transient pain or postembolization syndrome is a constellation of findings that are experienced to a variable degree, including pelvic pain and cramping, nausea and vomiting, low-grade fever, and general malaise. Frequently, symptoms of postembolization syndrome can be managed conservatively with oral analgesics and acetaminophen. However, aggressive management in the early postprocedure setting is advocated to increase patient comfort early during recovery so as to decrease the risk of deep venous thrombosis and pulmonary thromboembolic disease.

Transcervical expulsion of a leiomyoma occurs in 2.5% of cases (64). Leiomyoma expulsion may be associated with severe pelvic pain or cramping, recurrent bleeding, or infection (64). As stated earlier, submucosal leiomyomas are associated with an increased risk of transcervical expulsion. In most cases, an infarcted leiomyoma distends the endometrial canal and migrates toward the cervix; in some cases, dilatation of the internal os may be present. Spontaneous passage may occur, depending on the size of the infarcted leiomyoma (Fig 22). However, larger leiomyomas may require hysterectomy or hysteroscopic resection (Fig 23).

Other potential major complications include premature menopause (loss of ovarian function), bladder necrosis, and infection. Nontarget embolization can occur, resulting in loss of ovarian function or bladder necrosis; however, careful preprocedure planning and preembolization angiography greatly reduce this risk. Postembolization infection was one of the early complications but is now seen in less than 1% of patients after UFE (64).

Infectious complications include endometritis, tubo-ovarian abscess, pyomyoma, and uterine necrosis. Infectious endometritis occurs in 0.5% of women undergoing UFE (64). Most patients respond to antibiotics; however, in cases that do not respond to antibiotics, hysterectomy is required (64). At MR imaging, there may be enlargement of the uterus with an intracavitary hematoma that is of high signal intensity on T1-weighted images. Gas will appear as a signal void on both T1- and T2-weighted images (64).

Pelvic inflammatory disease and tubo-ovarian abscess are rare complications of UFE but should be considered in a patient with prolonged or recurrent pain and fever. Aggressive therapy with antibiotics and percutaneous drainage or surgery is required in cases that are refractory to medical therapy; therefore, recognition of imaging features is important. Often, the diagnosis is made on the basis of the clinical history and presenting features; however, in challenging cases, pelvic US is the initial imaging modality of choice for evaluation.

At US, a thick-walled unilocular or multilocular cystic adnexal mass with an associated hyperemic fallopian tube is diagnostic. At MR imaging, the signal intensity characteristics of a tubo-ovarian abscess may be similar to those of simple fluid, with low signal intensity on T1-weighted images

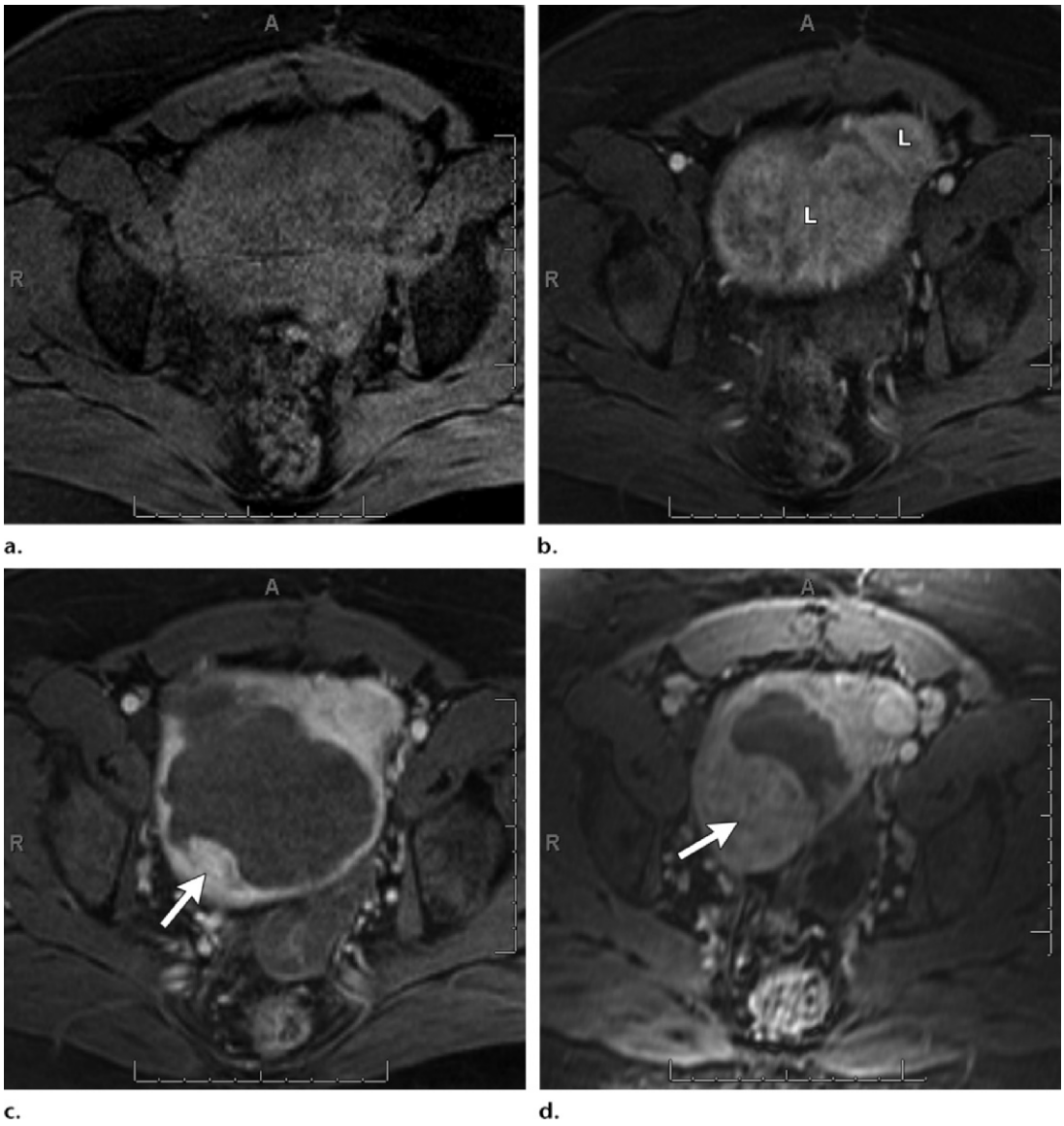

Figure 31. UFE failure due to regrowth. **(a, b)** Axial nonenhanced **(a)** and contrast-enhanced **(b)** fat-suppressed T1-weighted GRE images before UFE show two viable fundal leiomyomas (*L* in **b**). **(c)** Axial contrast-enhanced fat-suppressed T1-weighted GRE image after UFE shows residual viable tissue at the periphery of the larger leiomyoma (arrow) and homogeneous enhancement of the smaller leiomyoma. **(d)** Axial contrast-enhanced fat-suppressed T1-weighted GRE image obtained 3 months later shows regrowth of the large leiomyoma (arrow).

and high signal intensity on T2-weighted images. If proteinaceous material is present, there may be intermediate signal intensity on T1-weighted images and variable signal intensity on T2-weighted images. The abscess may be uni- or multilocular, and the abscess rim will typically be at least 3 mm thick (64), with enhancement of the rim after contrast material administration (Fig 32).

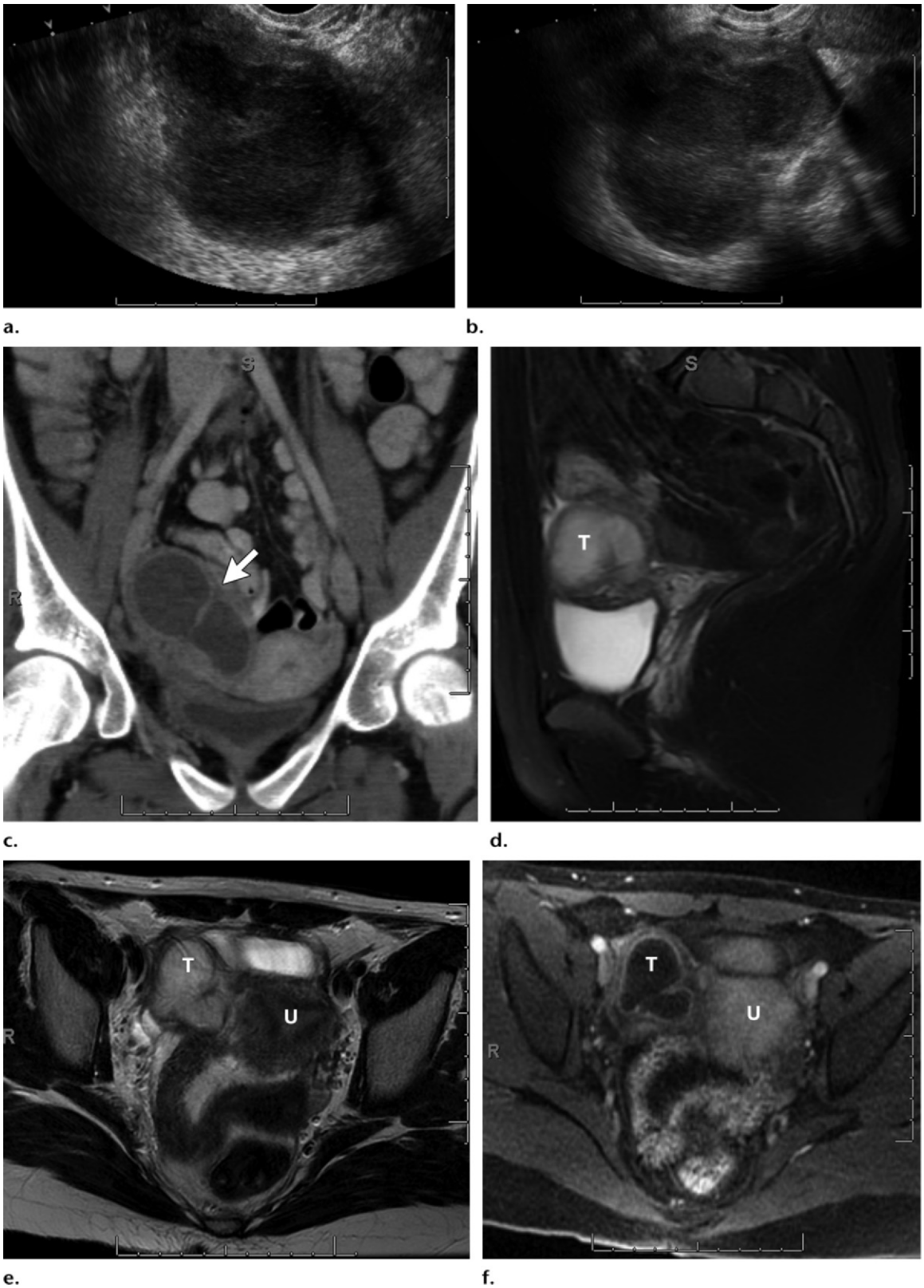

Figure 32. Tubo-ovarian abscess in a 37-year-old woman. **(a, b)** Sagittal **(a)** and coronal **(b)** endovaginal pelvic US images show a dilated, thick-walled, tubular structure that contains internal echoes in the right adnexa. **(c)** Coronal CT image obtained later the same day shows the dilated, thick-walled, tubular right adnexal structure with an incomplete septum (arrow) just lateral to the uterus. **(d–f)** Sagittal **(d)** and axial **(e)** T2-weighted and axial contrast-enhanced fat-suppressed T1-weighted GRE **(f)** images show the dilated, thick-walled, tubular right adnexal cystic structure *(T)* adjacent to the uterus (*U* in **e** and **f**) with rim enhancement after contrast material administration, findings consistent with a tubo-ovarian abscess.

Pyomyoma (aka suppurative leiomyoma) is a rare complication of UFE that occurs secondary to infarction and superimposed infection (Fig 23). After UFE, patients present with sepsis and no other source of infection. Imaging findings are not pathognomonic, as gas can be seen after UFE; therefore, correlation with clinical symptoms is critical (70,71).

Although uterine necrosis requiring hysterectomy occurs in less than 1% of UFE patients, contrast-enhanced MR imaging is the modality of choice for assessing the viability and vascularity of the myometrium (69). If uterine necrosis is present, there will be absence of myometrial enhancement on contrast-enhanced MR images (69).

Conclusions

Uterine leiomyoma is the most common tumor of the female reproductive system and accounts for the majority of hysterectomies in the United States. UFE is a safe and effective alternative to hysterectomy for relief from the symptoms of uterine leiomyomas. MR imaging performed before and after UFE is critical for demonstrating and localizing leiomyomas, assessing the likelihood of symptom relief after therapy on the basis of imaging characteristics, and monitoring the response of leiomyomas to therapy.

***Disclosures of Conflicts of Interest*.—D.G.M.:** *Related financial activities:* none. *Other financial activities:* consultant for CMC Contrast; expert witness in various legal medical malpractice cases.

References

1. Becker ER, Spalding J, DuChane J, Horowitz IR. Inpatient surgical treatment patterns for patients with uterine fibroids in the United States, 1998-2002. J Natl Med Assoc 2005;97(10):1336–1342.
2. Viswanathan M, Hartmann K, McKoy N, et al. Management of uterine fibroids: an update of the evidence. Evidence report/technology assessment no. 154, AHRQ publication no. 07-E011. Rockville, Md: Agency for Healthcare Research and Quality, 2007.
3. Parker WH. Myomectomy: laparoscopy or laparotomy? Clin Obstet Gynecol 1995;38(2):392–400.
4. Buttram VC Jr, Reiter RC. Uterine leiomyomata: etiology, symptomatology, and management. Fertil Steril 1981;36(4):433–445.
5. Rein MS, Barbieri RL, Friedman AJ. Progesterone: a critical role in the pathogenesis of uterine myomas. Am J Obstet Gynecol 1995;172(1 pt 1):14–18.
6. Goodwin SC, Vedantham S, McLucas B, Forno AE, Perrella R. Preliminary experience with uterine artery embolization for uterine fibroids. J Vasc Interv Radiol 1997;8(4):517–526.
7. Schwartz LB, Panageas E, Lange R, Rizzo J, Comite F, McCarthy S. Female pelvis: impact of MR imaging on treatment decisions and net cost analysis. Radiology 1994;192(1):55–60.
8. Jha RC, Ascher SM, Imaoka I, Spies JB. Symptomatic fibroleiomyomata: MR imaging of the uterus before and after uterine arterial embolization. Radiology 2000;217(1):228–235.
9. Katsumori T, Akazawa K, Mihara T. Uterine artery embolization for pedunculated subserosal fibroids. AJR Am J Roentgenol 2005;184(2):399–402.
10. Baird DD, Dunson DB, Hill MC, Cousins D, Schectman JM. High cumulative incidence of uterine leiomyoma in black and white women: ultrasound evidence. Am J Obstet Gynecol 2003;188(1):100–107.
11. Wise LA, Palmer JR, Harlow BL, et al. Reproductive factors, hormonal contraception, and risk of uterine leiomyomata in African-American women: a prospective study. Am J Epidemiol 2004;159(2):113–123.
12. Prayson RA, Hart WR. Pathologic considerations of uterine smooth muscle tumors. Obstet Gynecol Clin North Am 1995;22(4):637–657.
13. Gompel C, Silverberg SG. The corpus uteri. In: Gompel C, Silverberg SG, eds. Pathology in gynecology and obstetrics. Philadelphia, Pa: Lippincott, 1994; 163–283.
14. Novak ER, Woodruff JD. Myoma and other benign tumors of the uterus. In: Novak ER, Woodruff JD, eds. Novak's gynecologic and obstetric pathology. Philadelphia, Pa: Saunders, 1979; 260–279.
15. Okizuka H, Sugimura K, Takemori M, Obayashi C, Kitao M, Ishida T. MR detection of degenerating uterine leiomyomas. J Comput Assist Tomogr 1993;17(5):760–766.
16. Kim MD, Lee M, Jung DC, et al. Limited efficacy of uterine artery embolization for cervical leiomyomas. J Vasc Interv Radiol 2012;23(2):236–240.
17. Garcia CR, Tureck RW. Submucosal leiomyomas and infertility. Fertil Steril 1984;42(1):16–19.
18. Corson SL. Hysteroscopic diagnosis and operative therapy of submucous myoma. Obstet Gynecol Clin North Am 1995;22(4):739–755.
19. Ben-Baruch G, Schiff E, Menashe Y, Menczer J. Immediate and late outcome of vaginal myomectomy for prolapsed pedunculated submucous myoma. Obstet Gynecol 1988;72(6):858–861.
20. Panageas E, Kier R, McCauley TR, McCarthy S. Submucosal uterine leiomyomas: diagnosis of prolapse into the cervix and vagina based on MR imaging. AJR Am J Roentgenol 1992;159(3):555–558.

21. Hutchins FL Jr. Uterine fibroids: diagnosis and indications for treatment. Obstet Gynecol Clin North Am 1995;22(4):659–665.
22. Stewart EA. Uterine fibroids. Lancet 2001;357 (9252):293–298.
23. Hricak H, Tscholakoff D, Heinrichs L, et al. Uterine leiomyomas: correlation of MR, histopathologic findings, and symptoms. Radiology 1986;158(2): 385–391.
24. Dudiak CM, Turner DA, Patel SK, Archie JT, Silver B, Norusis M. Uterine leiomyomas in the infertile patient: preoperative localization with MR imaging versus US and hysterosalpingography. Radiology 1988;167(3):627–630.
25. Kawakami S, Togashi K, Konishi I, et al. Red degeneration of uterine leiomyoma: MR appearance. J Comput Assist Tomogr 1994;18(6):925–928.
26. Mittl RL Jr, Yeh IT, Kressel HY. High-signal-intensity rim surrounding uterine leiomyomas on MR images: pathologic correlation. Radiology 1991; 180(1):81–83.
27. Hricak H, Finck S, Honda G, Göranson H. MR imaging in the evaluation of benign uterine masses: value of gadopentetate dimeglumine-enhanced T1-weighted images. AJR Am J Roentgenol 1992;158 (5):1043–1050.
28. Novak ER, Woodruff JD. Adenomyosis (adenomyoma) uteri. In: Novak ER, Woodruff JD, eds. Novak's gynecologic and obstetric pathology. Philadelphia, PA: Saunders, 1979; 280–290.
29. Mark AS, Hricak H, Heinrichs LW, et al. Adenomyosis and leiomyoma: differential diagnosis with MR imaging. Radiology 1987;163(2):527–529.
30. Reinhold C, McCarthy S, Bret PM, et al. Diffuse adenomyosis: comparison of endovaginal US and MR imaging with histopathologic correlation. Radiology 1996;199(1):151–158.
31. Outwater EK, Siegelman ES, Van Deerlin V. Adenomyosis: current concepts and imaging considerations. AJR Am J Roentgenol 1998;170(2):437–441.
32. Togashi K, Ozasa H, Konishi I, et al. Enlarged uterus: differentiation between adenomyosis and leiomyoma with MR imaging. Radiology 1989;171 (2):531–534.
33. Scoutt LM, McCarthy SM, Lange R, Bourque A, Schwartz PE. MR evaluation of clinically suspected adnexal masses. J Comput Assist Tomogr 1994;18 (4):609–618.
34. Weinreb JC, Barkoff ND, Megibow A, Demopoulos R. The value of MR imaging in distinguishing leiomyomas from other solid pelvic masses when sonography is indeterminate. AJR Am J Roentgenol 1990;154(2):295–299.
35. Outwater EK, Siegelman ES, Talerman A, Dunton C. Ovarian fibromas and cystadenofibromas: MRI features of the fibrous component. J Magn Reson Imaging 1997;7(3):465–471.
36. Outwater EK, Siegelman ES, Kim B, Chiowanich P, Blasbalg R, Kilger A. Ovarian Brenner tumors: MR imaging characteristics. Magn Reson Imaging 1998;16(10):1147–1153.
37. Togashi K, Kawakami S, Kimura I, et al. Sustained uterine contractions: a cause of hypointense myometrial bulging. Radiology 1993;187(3):707–710.
38. Rha SE, Byun JY, Jung SE, et al. CT and MRI of uterine sarcomas and their mimickers. AJR Am J Roentgenol 2003;181(5):1369–1374.
39. Pattani SJ, Kier R, Deal R, Luchansky E. MRI of uterine leiomyosarcoma. Magn Reson Imaging 1995;13(2):331–333.
40. Janus CJ, White M, Dottino P, Brodman M, Goodman H. Uterine leiomyosarcoma: magnetic resonance imaging. Gynecol Oncol 1989;32(1):79–81.
41. Wegienka G, Baird DD, Hertz-Picciotto I, et al. Self-reported heavy bleeding associated with uterine leiomyomata. Obstet Gynecol 2003;101(3): 431–437.
42. Reich H. Laparoscopic myomectomy. Obstet Gynecol Clin North Am 1995;22(4):757–780.
43. Candiani GB, Fedele L, Parazzini F, Villa L. Risk of recurrence after myomectomy. Br J Obstet Gynaecol 1991;98(4):385–389.
44. Hartmann KE, Birnbaum H, Ben-Hamadi R, et al. Annual costs associated with diagnosis of uterine leiomyomata. Obstet Gynecol 2006;108(4):930–937.
45. Healy DL, Lawson SR, Abbott M, Baird DT, Fraser HM. Toward removing uterine fibroids without surgery: subcutaneous infusion of a luteinizing hormone-releasing hormone agonist commencing in the luteal phase. J Clin Endocrinol Metab 1986; 63(3):619–625.
46. Friedman AJ, Harrison-Atlas D, Barbieri RL, Benacerraf B, Gleason R, Schiff I. A randomized, placebo-controlled, double-blind study evaluating the efficacy of leuprolide acetate depot in the treatment of uterine leiomyomata. Fertil Steril 1989;51 (2):251–256.
47. West CP, Lumsden MA, Lawson S, Williamson J, Baird DT. Shrinkage of uterine fibroids during therapy with goserelin (Zoladex): a luteinizing hormone-releasing hormone agonist administered as a monthly subcutaneous depot. Fertil Steril 1987;48 (1):45–51.

48. Worthington-Kirsch RL, Popky GL, Hutchins FL Jr. Uterine arterial embolization for the management of leiomyomas: quality-of-life assessment and clinical response. Radiology 1998;208(3):625–629.
49. Spielmann AL, Keogh C, Forster BB, Martin ML, Machan LS. Comparison of MRI and sonography in the preliminary evaluation for fibroid embolization. AJR Am J Roentgenol 2006;187(6):1499–1504.
50. Siskin GP. Uterine fibroid embolization: successful patient selection is difficult, but makes all the difference. Endovascular Today. http://www.evtodayarchive.com/03_archive/1102/071.html. Accessed March 15, 2008.
51. Verma SK, Bergin D, Gonsalves CF, Mitchell DG, Lev-Toaff AS, Parker L. Submucosal fibroids becoming endocavitary following uterine artery embolization: risk assessment by MRI. AJR Am J Roentgenol 2008;190(5):1220–1226.
52. Shlansky-Goldberg RD, Coryell L, Stavropoulos SW, et al. Outcomes following fibroid expulsion after uterine artery embolization. J Vasc Interv Radiol 2011;22(11):1586–1593.
53. Radeleff B, Eiers M, Bellemann N, et al. Expulsion of dominant submucosal fibroids after uterine artery embolization. Eur J Radiol 2010;75(1):e57–e63.
54. Nikolaidis P, Siddiqi AJ, Carr JC, et al. Incidence of nonviable leiomyomas on contrast material-enhanced pelvic MR imaging in patients referred for uterine artery embolization. J Vasc Interv Radiol 2005;16(11):1465–1471.
55. Kroencke TJ, Scheurig C, Poellinger A, Gronewold M, Hamm B. Uterine artery embolization for leiomyomas: percentage of infarction predicts clinical outcome. Radiology 2010;255(3):834–841.
56. Pelage JP, Jacob D, Fazel A, et al. Midterm results of uterine artery embolization for symptomatic adenomyosis: initial experience. Radiology 2005;234(3):948–953.
57. Parazzini F, Vercellini P, Panazza S, Chatenoud L, Oldani S, Crosignani PG. Risk factors for adenomyosis. Hum Reprod 1997;12(6):1275–1279.
58. Matalliotakis IM, Kourtis AI, Panidis DK. Adenomyosis. Obstet Gynecol Clin North Am 2003;30(1):63–82.
59. Bazot M, Cortez A, Darai E, et al. Ultrasonography compared with magnetic resonance imaging for the diagnosis of adenomyosis: correlation with histopathology. Hum Reprod 2001;16(11):2427–2433.
60. Kitamura Y, Allison SJ, Jha RC, Spies JB, Flick PA, Ascher SM. MRI of adenomyosis: changes with uterine artery embolization. AJR Am J Roentgenol 2006;186(3):855–864.
61. Jha RC, Takahama J, Imaoka I, et al. Adenomyosis: MRI of the uterus treated with uterine artery embolization. AJR Am J Roentgenol 2003;181(3):851–856.
62. Tamai K, Koyama T, Saga T, et al. The utility of diffusion-weighted MR imaging for differentiating uterine sarcomas from benign leiomyomas. Eur Radiol 2008;18(4):723–730.
63. Pelage JP, Cazejust J, Pluot E, et al. Uterine fibroid vascularization and clinical relevance to uterine fibroid embolization. RadioGraphics 2005;25(spec no):S99–S117.
64. Kitamura Y, Ascher SM, Cooper C, et al. Imaging manifestations of complications associated with uterine artery embolization. RadioGraphics 2005;25(Spec No.):S119–S132.
65. Spies JB, Bruno J, Czeyda-Pommersheim F, Magee ST, Ascher SA, Jha RC. Long-term outcome of uterine artery embolization of leiomyomata. Obstet Gynecol 2005;106(5 pt 1):933–939.
66. Edwards RD, Moss JG, Lumsden MA, et al. Uterine-artery embolization versus surgery for symptomatic uterine fibroids. N Engl J Med 2007;356(4):360–370.
67. Pelage JP, Guaou NG, Jha RC, Ascher SM, Spies JB. Uterine fibroid tumors: long-term MR imaging outcome after embolization. Radiology 2004;230(3):803–809.
68. Worthington-Kirsch RL, Spies JB, Myers ER, et al. The Fibroid Registry for outcomes data (FIBROID) for uterine embolization: short-term outcomes. Obstet Gynecol 2005;106(1):52–59.
69. Verma SK, Gonsalves CF, Baltarowich OH, Mitchell DG, Lev-Toaff AS, Bergin D. Spectrum of imaging findings on MRI and CT after uterine artery embolization. Abdom Imaging 2010;35(1):118–128.
70. Worthington-Kirsch RL, Hutchins FL Jr, Berkowitz RP. Uterine interstitial gas after uterine artery embolization: a benign finding. J Vasc Interv Radiol 1999;14:181–185.
71. Shukla PA, Kumar A, Klyde D, Contractor S. Pyomyoma after uterine artery embolization. J Vasc Interv Radiol 2012;23(3):423–424.

RadioGraphics

Role of MR Imaging of Uterine Leiomyomas before and after Embolization

Sandeep P. Deshmukh, MD • Carin F. Gonsalves, MD • Flavius F. Guglielmo, MD • Donald G. Mitchell, MD

RadioGraphics 2012; 32:E251–E281 • **Published online** 10.1148/rg.326125517 • **Content Codes:** GU IR MR OB

Page E252
However, MR imaging is the most accurate imaging modality for detection and localization of leiomyomas and their mimics: adenomyosis, solid adnexal masses, focal myometrial contractions, and occasionally uterine leiomyosarcomas.

Page E252
Over time, preprocedure MR imaging is the diagnostic tool of choice for determining patient eligibility for UFE and for assessing potential procedural risk. Furthermore, MR imaging is also a useful tool for determining treatment outcome and for diagnosing potential complications after UFE.

Page E267
Preprocedure MR imaging has also proved useful in assessing the success of UFE, as well as assessing potential risks for complications.

Page E267
Preprocedure MR imaging can help predict which leiomyomas are more likely to become intracavitary after the procedure.

Page E274
The location, size, and enhancement of leiomyomas provide significant prognostic information about the potential success of UFE. Therefore, the location, size, size of the stalk (if pedunculated), and enhancement characteristics of leiomyomas should be analyzed and reported.